Molecular Pharmacology Fast Forward. Published on August 14, 2008 as doi:10.1124/mol.108.050161

Mitochondria dependent ROS-mediated programmed cell death (PCD) induced by 3,3'-Diindolylmethane (DIM) through Inhibition of FoF1-ATP Synthase in unicellular protozoan parasite *Leishmania donovani*

Amit Roy, Agneyo Ganguly, Somdeb BoseDasgupta, Benu Brata Das, Churala Pal, Parasuraman Jaisankar, and Hemanta K. Majumder

Molecular Parasitology Laboratory (A.R., A.G., S.B., H.K.M.) and Department of Medicinal Chemistry (C.P., P.J.), Indian Institute of Chemical Biology, 4, Raja S.C Mullick Road, Kolkata –700032, INDIA, and Laboratory of Molecular Pharmacology (B.B.D.), NCI, NIH, Bethesda, MD 20892-4255, USA

Molecular Pharmacology Fast Forward. Published on August 14, 2008 as DOI: 10.1124/mol.108.050161
This article has not been copyedited and formatted. The final version may differ from this version.

Running Title: 3,3'-Diindolylmethane (DIM), a FoF1-ATP synthase inhibitor

Address correspondence to: Hemanta K. Majumder, Molecular Parasitology Laboratory, Indian Institute of Chemical Biology, 4, Raja S.C. Mullick Road, Kolkata-700032, India.

E-mail: hkmajumder@iicb.res.in

The number of text pages: 51.

The number of Tables: 2.

The number of Figures: 11.

The number of References: 41.

The number of words in the Abstract: 235.

The number of words in the Introduction: 727.

The number of words in the Discussion: 1488.

Supplementary Information

No. of Supplementary Tables: 2

No. of Supplementary Figures: 2.

The abbreviations used: PCD, programmed cell death; ROS, reactive oxygen species; DIM, 3,3'-Diindolylmethane; CPT, camptothecin; PBS, phosphate-buffered saline; CCCP, carbonyl cyanide m-chloro-phenylhydrazone; NAC, N-acetyl-L-cysteine; SB, sodium benzoate; BHT, butylated hydroxy toluene.

Molecular Pharmacology Fast Forward. Published on August 14, 2008 as DOI: 10.1124/mol.108.050161
This article has not been copyedited and formatted. The final version may differ from this version.

Abstract:

Mitochondria are the principal site for the generation of cellular ATP by oxidative phosphorylation. FoF1-ATP synthase, a complex V of electron transport chain, is an important constituent of mitochondria dependent-signaling pathways involved in apoptosis. In the present study, we have shown for the first time that 3,3'-Diindolylmethane (DIM), a DNA topoisomerase I poison inhibits mitochondrial FoF1-ATP synthase of *Leishmania donovani* and induces programmed cell death (PCD), which is a novel insight into the mechanism in protozoan parasites. DIM-induced inhibition of FoF1-ATP synthase activity causes depletion of mitochondrial ATP levels and significant stimulation of mitochondrial ROS production, followed by depolarization of mitochondrial membrane potential ($\Delta\Psi m$). Since, $\Delta\Psi m$ is the driving force for mitochondrial ATP synthesis, loss of $\Delta\Psi m$ results in depletion of cellular ATP level. The loss of $\Delta\Psi m$ causes the cellular ROS generation and in turn led to the oxidative DNA lesions followed by DNA fragmentation. On the other hand, loss of $\Delta\Psi m$ leads to release of cytochrome c into the cytosol and subsequently activates the caspase-like proteases, which lead to oligonucleosomal DNA cleavage. We have also shown that mt-DNA depleted cells are insensitive to DIM to induce PCD. Therefore, mitochondria are necessary for cytotoxicity of DIM in kinetoplastid parasites. Taken together, our studies indicate for the first time that DIM-induced mitochondrial dysfunction by inhibition of FoF1-ATP synthase activity leads to PCD in *Leishmania* parasites, which could be exploited to develop newer potential therapeutic targets.

Molecular Pharmacology Fast Forward. Published on August 14, 2008 as DOI: 10.1124/mol.108.050161
This article has not been copyedited and formatted. The final version may differ from this version.

Introduction:

Apoptosis, a form of programmed cell death (PCD), is a genetically regulated active physiological process of cell suicide that causes cell deletion without inflammation, scarring or release of cellular contents. Mitochondria of living cells play a pivotal role in controlling life and death (Green et al., 1998). Mitochondrion is an important cellular source for the generation of reactive oxygen species (ROS) inside the cells (Halliwell and Gutteridge, 1990). Maintenance of proper mitochondrial transmembrane potential ($\Delta\Psi m$) is essential for the survival of the cell as it derives the synthesis of ATP and maintains oxidative phosphorylation (Gottlieb, 2001).

3,3'-Diindolylmethane (DIM) is a major acid condensation product of Indole-3-Carbinol (I3C), a natural compound found in vegetables of the genus *Brassica* plants. It has an anti-carcinogenic effect and inhibits the growth of human cancer cells. DIM induced G_1 cell cycle arrest occurs by up-regulation of p21 in breast cancer cells (Hong et al., 2002). DIM significantly inhibits TNF-α induced translocation of NF-$\kappa\beta$ to the nucleus and down regulates NF-$\kappa\beta$ function and promotes apoptotic signaling (Rahman and Sarkar, 2005). DIM is a mitochondrial H^+-ATP synthase inhibitor that can induce $p21^{CIP/Waf1}$ expression in human breast cancer cells (Gong et al., 2006). Recently, we have shown that DIM binds at topoisomerase I-DNA interface and trap the cleavable complexes by preventing the religation step. DIM also interacts with both free enzyme and substrate DNA and acts as a non-competitive topoisomerase I inhibitor (Roy et al., 2008).

Leishmania donovani, a unicellular protozoan parasite, is responsible for visceral leishmaniasis or “Kala-azar” in humans worldwide. The organism has a digenic life cycle residing as flagellated extracellular promastigotes in the gut of insect vector and as non-flagellated amastigotes in mammalian host macrophages. Recently, various new compounds

Molecular Pharmacology Fast Forward. Published on August 14, 2008 as DOI: 10.1124/mol.108.050161
This article has not been copyedited and formatted. The final version may differ from this version.

have been developed as anti-leishmanial drugs. The pentavalent antimonial sodium stibogluconate (SAG) is the first line of drugs for visceral leishmaniasis. This compound has variable efficacy and toxic side effects. The second line of drugs, amphotericin B and pentamidine are used clinically, which have some limited efficacy and are very toxic (Iwu et al., 1994). For that reasons, improved drug therapy of *Leishmania* infections is still desirable and the need for newer molecular targets and intervention strategies is clear and justified. PCD was reported in unicellular protozoan parasite *L. donoivani* induced by CPT (Sen et al., 2004a), withaferin A (Sen et al., 2007a) and H_2O_2 (Das et al., 2001) etc. The characterization of cellular events associated with PCD is necessary to find out the cellular targets, which might be exploited in these protozoan parasites. In search for such strategies, FoF1-ATP synthase of *Leishmania* offers as an attractive target. Mitochondrial FoF1-ATPase/ATP synthase is a ubiquitous enzyme that is responsible for synthesis of ATP and therefore, it is critical for cell growth and survival. Resveratrol and isoflavones (e.g., genistein) inhibited the mitochondrial F0F1-ATPase/ATP synthase. Piceatannol, a stilbene phytochemical, inhibits mitochondrial FoF1-ATPase activity and is more potent than resveratrol and isoflavones (Zheng and Ramirez, 1999). Apoptolidin, a selective cytotoxic agent is an inhibitor of FoF1-ATP synthase (Salomon et al., 2001). Atrazine, a widely used triazine herbicide inhibits mitochondrial functions of sperm through F1Fo-ATP synthase (Hase et al., 2008).

In the present study, we have shown for the first time that DIM, a potent topoisomerase I poison (Roy et al., 2008), is a potent inhibitor of mitochondrial FoF1-ATP synthase in *Leishmania* parasites. Unlike higher eukaryotes, inhibition of FoF1-ATP synthase activity inside cells is sufficient to induce PCD in *Leishmania* parasites. We have analyzed nuclear, mitochondrial and cytosolic changes associated with apoptosis through inhibition of FoF1-ATP

Molecular Pharmacology Fast Forward. Published on August 14, 2008 as DOI: 10.1124/mol.108.050161
This article has not been copyedited and formatted. The final version may differ from this version.

synthase that causes mitochondrial membrane depolarization. Loss of mitochondrial membrane potential ($\Delta\Psi m$) leads to release of cytochrome c into the cytosol, which leads to activation of both CED3/CPP32 and ICE group of proteases inside cells. Taken together, our results provide for the first time an insight into the mitochondria dependent apoptotic like death pathway induced by DIM in *Leishmania* parasites through inhibition of FoF1-ATP synthase activity and alterations in mitochondrial as well as cellular ATP level. The depletion of ATP level enhances apoptosis by creating a cellular oxidative stress followed by DNA fragmentation in leishmanial cells. Since, this FoF1-ATP synthase enzyme is a potent target we have studied the effect of DIM on this ubiquitous enzyme. Such information has great potential in determining the role of mitochondria in apoptosis-like death of leishmanial cells and help in designing of better drugs for leishmaniasis.

Molecular Pharmacology Fast Forward. Published on August 14, 2008 as DOI: 10.1124/mol.108.050161
This article has not been copyedited and formatted. The final version may differ from this version.

Materials and Methods:

Chemicals: The bioactive DIM (3, 3'-Diindolylmethane; $C_{17}H_{14}N_{2)}$ was synthesized chemically from Indole and Urotropine as described previously (Roy et al., 2008). Camptothecin (CPT) purchased from Sigma Chemicals (St.Louis, MO, USA) was dissolved in 100% Dimethyl sulphoxide (DMSO) at 20 mM concentration and stored at -20^0C. NAC, SB, Mannitol and BHT purchased from Sigma Chemicals (St.Louis, MO, USA) and were dissolved in 100% DMSO at 50 mM and stored at -20^0C.

Parasite Culture and maintenance: *Leishmania donovani* strain AG83 promastigotes were grown at 22^0C in Rays modified media and in M199 liquid media supplemented with 10% fetal calf serum (FCS) as described previously (Mittra et al., 2000).

Cell Viability Test by MTT assay: The effect of drug on the viability of *L.donovani* AG83 cells is determined by 3-(4,5-dimethylthiazol-2-yl)-2,5-diphenylterazolium bromide (MTT) assay (Mosman et al., 1983). The cells at the exponential phase were collected and transferred into 24 well plate (about 4 X 10^5 to 10^6 cells per well). The cells were then incubated for 12 h in the presence of various concentrations of DIM. After incubation the cells were centrifuged and the supernatant was aspirated. The cell pellet was washed with PBS (1X) twice and then finally suspended in 100 µl of PBS (1X) in 96 well plates. Ten (10) µl of MTT solution (10 µg/ml) was added in each sample of 96 well plates and was incubated for 4 hours. After incubation 100 µl of stop solution (stock: 4963 µl isopropanol and 17 µl concentrated HCl) was added and kept for 20 minutes at room temperature. The O.D. was taken at A_{570} on an ELISA reader.

Isolation of Mitochondria: Mitochondrial vesicles were isolated from *L.donovani* promastigotes by hypotonic lysis and Percoll centrifugation as described previously (Harris et al., 1990). All operations were carried out at 0-4°C. Promastigotes were harvested, washed with PBS

Molecular Pharmacology Fast Forward. Published on August 14, 2008 as DOI: 10.1124/mol.108.050161
This article has not been copyedited and formatted. The final version may differ from this version.

(1X) containing 20 mM glucose, and suspended in hypotonic lysis buffer (1 mM Tris-HCl, pH 8.0, 1 mM EDTA) at 2.0 X 10^9 cells/ml. The suspension was homogenized with 5 strokes of a type B pestle in an all-glass Kontes homogenizer. Cells were lysed by forceful passage of the homogenate through a 26-gauge hypodermic needle. Lysis was monitored microscopically. Sucrose (2.0 M stock) was immediately added to the lysate to 0.25 M, and the lysate centrifuged at 11,500 rpm in a Sorvall SS34 rotor. The pellet was suspended in one-fifth volume of the original lysate in STM buffer (0.25 M sucrose, 20 mM Tris- HCl, pH 8.0, 2 mM $MgCl_2$, 0.1 mM PMSF). The lysate was diluted 5-fold with STE-A buffer (0.25M sucrose, 20 mM Tris-HCl, pH 8.0, 2 mM EDTA, 0.1 mM PMSF) and centrifuged. The pellet of crude mitochondria was resuspended in one-fifth volume of STE-A, layered on a 20- 35% Percoll gradient, and centrifuged at 24,000 rpm in a Beckman SW28 rotor for 45 min. The turbid band of purified mitochondria near the bottom of the tube was withdrawn, washed 4 times with STE-B (0.25 M sucrose, 10 mM Tris-HCl, pH 7.5, 1 mM EDTA, 0.1 mM PMSF), and suspended in storage buffer (50% glycerol, 0.25 M sucrose, 10 mM Tris-HCl, pH 7.5, 1 mM EDTA, 0.1 mM PMSF) at a protein concentration of 7-8 mg/ml. Mitochondria were stored at -20^0C.

PK/LDH-coupled ATPase assay: Fresh isolated mitochondria were solubilized in 1% digitonin solubilizing buffer containing 50 mM Tris-HCl (pH 7.4), 120 mM NaCl, 5 mM KCl, 1 mM $MgSO_4$, 1 mM $CaCl_2$, and 10% glycerol for 30 minutes at 4^0C. The ATPase activity of solubilized mitochondria was measured spectrophotometrically at 340 nm by coupling the production of ADP to the oxidation of NADH via pyruvate kinase and lactate dehydrogenase as described previously (Gong et al., 2006). The reaction mixture contained a final volume of 400 µl at 25^0C and included the following: 100 mM Tris-HCl (pH 8.0), 2 mM ATP, 2 mM $MgCl_2$, 50 mM KCl, 0.2 mM EDTA, 0.2 mM NADH, 1 mM phosphoenolpyruvate (PEP), 5 units pyruvate

Molecular Pharmacology Fast Forward. Published on August 14, 2008 as DOI: 10.1124/mol.108.050161
This article has not been copyedited and formatted. The final version may differ from this version.

kinase, 8 units lactate dehydrogenase, 10 µM cyanide, 10 µM rotenone, 10 µM antimycin A and 25 to 50 µg mitochondrial proteins. These assay conditions minimized the contribution of other transport ATPases, such as Na^+,K^+-ATPase. Test compounds were added before the reaction was started by addition of 25 to 50 µg of solubilized mitochondria at a constant temperature of 25^0C.

Measurement of complex I, II, III, and IV activities: All the assays were performed as described previously (Sen et al., 2006). The activity of complex I was assayed using ferricyanide as the electron acceptor. The reaction was initiated by the addition of mitochondrial suspension (10–30 µg protein) in 50 mM phosphate buffer, pH 7.4 containing 0.17 mM NADH, 0.6 mM ferricyanide and Triton X-100 (0.1% v/v) at 30^0C and the rate of oxidation of NADH was measured by the decrease in absorbance at 340 nm.

Succinate–CoQ reductase (complex II) activity was assayed in 50 mM KH_2PO_4 buffer (pH 7.4) containing 100 µM EDTA, 0.1% Triton X-100, 20 mM potassium succinate, 10 µM cyanide, 10 µM rotenone, and 10 µM antimycin A. After preincubation at 30^0C for 10 min ubiquinone 2 (50 µM) and 2,6-dichlorophenol-indophenol (DCIP; 75 µM) were added and the reduction of DCIP was measured at 600 nm.

The activity of complex III was assayed in 50 mM KH_2PO_4 buffer (pH 7.4) containing 1 mM EDTA, 50 µM oxidized cytochrome c, 2 mM KCN, and 10 µM rotenone. After the addition of ubiquinol 2 (150 µM) the rate of reduction of cytochrome c was measured at 550 nm and antimycin A (10 µM) was added to determine the background rate.

The activity of complex IV was assayed by following the oxidation of reduced cytochrome c (ferrocytochrome c) at 550 nm. Reduced cytochrome c (50 µM) in 10 mM phosphate buffer pH 7.4 was added in each of 1ml cuvettes. In the blank cuvette ferricyanide (1 mM) was added to oxidize ferrocytochrome c and the reaction was initiated in the sample cuvette

Molecular Pharmacology Fast Forward. Published on August 14, 2008 as DOI: 10.1124/mol.108.050161
This article has not been copyedited and formatted. The final version may differ from this version.

by the addition of mitochondrial suspension (10–30 µg protein). The rate of decrease of absorbance at 550 nm was measured at room temperature.

Preparation of cytoplasmic extract: Cytoplasmic extracts were prepared both in treated and untreated *Leishmania* cells as described previously (Sen et al., 2004b). Briefly, the cells (2.5 X 10^7) after different treatments were harvested suspended in cell extraction buffer (20 mM HEPES-KOH, 10 mM KCl, 1.5 mM MgCl2, 1 mM EDTA, 1 mM DTT, 200 µM PMSF, 10 µg/ml leupeptin and pepstatin) and lysed by a process of freeze-thaw using nitrogen cavitations and a 37^0C water bath simultaneously. Then lysate was centrifuged at 10,000xg for 1 h, and supernatants were used as a source of cytoplasmic extract.

Measurement of cellular ATP level: ATP content was determined by the Luciferin/Luciferase method as described previously (Sen et al., 2006). The assay is based on the requirement of luciferase for ATP in producing light (emission maximum 560 nm at pH 7.8). Briefly, the cells (3 X 10^7) were treated with different concentrations of drugs for the indicated times and washed with PBS (1X) twice and suspended in PBS (1X). The mitochondrial and cytosolic extracts were prepared as above. An aliquot of these fractions were assayed for ATP using the luciferase ATP assay kit (Sigma chemical). The amount of ATP in the experimental samples was calculated from standard curve prepared with ATP and expressed as percentage of ATP in cells.

Measurement of mitochondrial membrane potential ($\Delta\psi_m$): Mitochondrial transmembrane potential was investigated using JC1 dye, a fluochrome. This dye accumulates in the mitochondrial matrix under the influence of $\Delta\psi_{m,}$ where it reversibly forms monomers (green) with characteristic absorption and emission spectra. (Sen et al., 2004b). Briefly, the leishmanial cells after different treatment with DIM were harvested and washed with PBS (1X). The cells were then incubated at 37°C in 5% CO_2 incubator for 1 hour with a final concentration of JC1

Molecular Pharmacology Fast Forward. Published on August 14, 2008 as DOI: 10.1124/mol.108.050161
This article has not been copyedited and formatted. The final version may differ from this version.

dye at 5 μg/μl. Cells were then analyzed by fluorescence measurement through spectrofluorometer using 507 nm as excitation and 530 nm as emission wavelengths and 507 nm as excitation and 590 nm as emission wavelengths to analyze $\Delta\psi_{m.}$ Spectrofluorometeric data presented here are representative of three experiments. The ratio of the reading at 590 nm to the reading at 530 nm (590:530 ratio) was considered as the relative $\Delta\psi_m$ value.

Measurement of ROS level: We have isolated mitochondria and cytosol from the same DIM treated cells and measured the ROS from mitochondrial and cytosolic fractions. To analyze the mitochondrial ROS production, isolated mitochondria were suspended in 500-μl analysis buffer [250 mM sucrose, 20 mM 3-(N-morpholino) butane sulfonic acid, 10 mM Tris-base, 100 μM KH_2PO_4, 0.5 mM Mg^{2+}, 1 μM cyclosporin A (pH 7.0)] containing 5 mM succinate and 1 μg/ml CM-H_2DCFDA (Sen et al., 2004b). In some samples, oligomycin (10 μM), a complex V classical inhibitor was added to enhance ROS production. Mitochondria suspension were incubated at room temperature, protected from light for 30 minutes and then analyzed by spectrofluorometer using 507 nm as excitation and 530 nm as emission wavelengths. To analyze the cytosolic ROS production, isolated cytosolic fractions were incubated with CM-H_2DCFDA for 30 minutes and then analyzed by spectrofluorometer using 507 nm as excitation and 530 nm as emission wavelengths.

Intracellular ROS level was measured in DIM treated and untreated leishmanial cells as described previously (Sen et al., 2004b). Briefly, cells (approximately, 2.5 X 10^7 cells) after different time periods with DIM and some antioxidants (NAC, SB, Mannitol) treatments were washed and resuspended in 500 μl of medium 199 and were loaded with a cell-permeate probe H_2DCFDA for 1h. It is a nonpolar compound and gets hydrolyzed within the cell to form a non-fluorescent derivative, which in presence of a proper oxidant converted to a fluorescent product.

Fluorescence was measured through spectrofluorometer using 507 nm as excitation and 530 nm as emission wavelengths. For all measurements basal fluorescence was substractred. Spectrofluorometeric data presented here are representative of three experiments.

Measurement of GSH level: GSH level was measured by monochlorobimane (MCB) dye that gives a blue fluorescence when bound to glutathione (Sen et al., 2004a). *L. donovani* promastigotes (approximately, 10^6 cells) were treated with or without DIM at different times. The cells were then pelleted down and lysed by cell lysis buffer according to the manufacturer's protocol (Apo Alert^{TM} glutathione assay kit). Cell lysates were incubated with MCB (2 mM) for 3 hr at 37^0C. The decrease in glutathione levels in the extracts of nonapoptotic and apoptotic cells were detected by fluorometer with 395 nm excitation and 480 nm emission wavelengths. Spectrofluorometeric data presented here are representative of three experiments.

Measurement of total fluorescent lipid peroxidation product: DIM treated and untreated *L.donovani* cells were pelleted down and washed twice with 1X PBS. The pellet was dissolved in 2 ml of 15% SDS-PBS solution. The fluorescence intensities of the total fluorescent lipid peroxidation products were measured with excitation at 360 nm and emission at 430 nm and expressed as relative fluorescence units with respect to quinine sulphate (1mg/ml in 0.5 M H_2SO_4) (Sen et al., 2004a). Spectrofluorometeric data presented here are representative of three experiments.

Detection of cytochrome c release by western blotting: DIM treated and untreated cells were harvested and washed twice with 1X PBS, suspended in cell fractionation buffer (Apo Alert^{TM} cell fractionation kit) and homogenized. After the separation of cytosolic and mitochondrial fraction, 50 μg each of cytosolic proteins were separated on 12% SDS-PAGE and

immunoblotted with the rabbit polyclonal cytochrome c antibody. HRP conjugated secondary antibody was used and protein band was visualized by DAB color reaction.

Determination of caspase-like protease activity: *L. donovani* promastigotes (approximately, 10^6 cells) was treated with or without DIM for different time periods. The cells were then pelleted and lysed by cell lysis buffer according to the manufacturer's protocol (Apo Alert™ caspase assay kit). Cell lysates were incubated with respective caspase buffers to detect CED3/CPP32 group of protease activity. A fluorogenic peptide substrates, DEVD-AFC at 100 μM and 1X reaction buffer containing 100 mM DTT was added to corresponding cell lysates to measure the activity of CED3/CPP32 group of proteases. In parallel set of reactions, 1 μl of CED-3/CPP32 group of protease inhibitor was added to the reaction prior to the addition of cell lysates. AFC release was measured after incubating those samples at 37^0C for 2 hours by fluorometer with 380 nm excitation and 460 nm emissions respectively. Spectrofluorometeric data presented here are representative of three experiments.

Assay of PARP cleavage: Cell lysates were prepared from DIM-treated and untreated cells, separated on 12% SDS-PAGE and subjected to western blot analysis as described previously (Sen et al., 2004a). Anti-PARP polyclonal antibody was diluted to 1000 times and HRP conjugated secondary antibody was used to visualize the reactive band by DAB colour reaction.

Double staining with annexin V and propidium iodide: Externalization of phosphatidylserine on the outer membrane of untreated and DIM-treated promastigotes was measured by the binding of annexin V-FITC and PI using an annexin V-FLUOS staining kit (Roche Diagnostics). Cells were visualized with TCS-SP Leica confocal microscope through dual FITC/PI filter set. Total cells versus annexin V-labeled cells were calculated and data expressed as percentage of

Molecular Pharmacology Fast Forward. Published on August 14, 2008 as DOI: 10.1124/mol.108.050161
This article has not been copyedited and formatted. The final version may differ from this version.

apoptotic cells. It should be noted that 100 cells per group with identical morphology were calculated for each condition.

Flow cytometric analysis: *L.donovani* promastigotes were treated with DIM (15 μM) for different time and washed twice with PBS. The cells then resuspended in 100 μl of binding buffer provided with the apoptosis detection kit (Roche Diagnostics). The cells were stained with annexinV-FITC antibody and PI as per instructions given by the manufacturer, and scanned for fluorescence intensity of cell population in different quadrants. The fraction of cell population in different quadrants was analyzed using quadrant statistics. The cells in the lower right quadrant represented apoptosis and in the upper right quadrant represented post apoptotic necrosis.

DNA fragmentation assay for detection of apoptosis: Cells were cultured in 24-well plates and treated with drugs for different times. Samples were collected at requisite time points and subjected to measurement of DNA fragmentations by detecting the cytoplasmic histone-associated DNA fragments (mononucleosome and oligonucleosomes) formed during apoptosis using a cell death detection ELISA kit (Roche Biochemicals) according to the manufacturer's protocol. DNA fragmentation was detected by spectrophotometric measurement of microtiter plates in a Thermo MULTISKAN EX plate reader at 405 nm, and relative percentages (with respect to samples treated with micrococcal nuclease and normalized to percentage values) were plotted as units of time or drug concentrations.

Development of mitochondrial DNA depleted parasites: *L. donovani* AG 83 promastigote cells were treated with 20 μM berenil for 24 h as described previously (Shapiro et al., 1989). Smears of treated promastigotes (approximately10^7cells) were assessed for dyskinetoplastidy by ethidium bromide staining (0.1 μg/ml in 1X phosphate buffered saline containing 10% glycerol).

The cells were viewed with a TCS-SP Leica confocal microscope system equipped with a krypton-argon mixed laser.

Measurement of *in vivo* DNA synthesis: Exponentially growing *L. donovani* promastigote cells (6 x 10^{6} cells /ml) were radiolabeled by adding [*methyl*-^{3}H] thymidine (Amersham) into the medium M199 supplemented with 10% heat inactivated fetal bovine serum (FBS) to a final concentration of 5 μCi/ml and incubated for 8-24 h at 22^{0}C in presence or absence of different concentrations of DIM. Following incubation, cells were lysed with 10% trichloroacetic acid (TCA) and harvested in a Skatron Combi cell harvester. The incorporation of radioactivity in acid-precipitable DNA was measured in a liquid scintillation counter as described previously (Chowdhury et al., 2002).

Cell Cycle Analysis: For flow cytometry analysis of DNA content, exponentially grown *L.donovani* promastigote cells (2.5 X 10^{6} cells) were treated with DIM (15 μM) for 2, 4 and 6 h. The cells were then harvested and washed three times with PBS (1X), fixed in 45% ethanol (diluted in 1X PBS), treated with 500 μg/ml RNAse A and then suspended in 0.5 M sodium citrate containing 69 μM PI. These samples were incubated for 45 minutes in the dark at room temperature and were analyzed through flow cytometry. The cells (20,000) were analyzed from each sample. The percentage of cells in G1, S and G2/M phases of the cell cycle were determined by multicycle computer software.

Statistical analysis: The data was expressed as mean $\pm$ SD unless mentioned. Comparisons were made between different treatments using unpaired Student's t test.

Molecular Pharmacology Fast Forward. Published on August 14, 2008 as DOI: 10.1124/mol.108.050161
This article has not been copyedited and formatted. The final version may differ from this version.

Results:

DIM inhibits growth of *L.donovani* promastigotes and amastigotes and reduces parasite burden.

L. donovani AG83 promastigotes (3.0 X 10^6 cells/ml) were incubated with five different concentrations of DIM (1, 5, 10, 15 and 20 μM) for 2, 4, 8 and 12 h, following which the numbers of live promastigotes were counted by MTT assay (Fig. 1A). At 8 h, 95% growth was inhibited by 15 μM DIM, which was comparable to the inhibition (98%) achieved by 20 μM DIM at 4 h and 100% growth was inhibited by 15 μM DIM at 12 h, which was comparable to the inhibition achieved by 20 μM DIM at 8 h. Consistent with these results it was observed that after 12 h treatment with 15 μM DIM, growth of *L.major, L.tropica* and *L.tarentolae* promastigotes were inhibited to the extent of 92 %, 90% and 94%, respectively (Fig. 1B). The human macrophage cells (U937) were infected with *L.donovani* AG83 promastigotes *in vitro*. Infected macrophages, after subsequent washing were incubated with same concentrations of DIM for 12 h (Fig. 1C). The IC_{50} values of DIM were calculated to be 1.2 μM and 2.5 μM at 12 h in promastigotes and amastigotes, respectively. We have also checked the inhibition of parasite burden in animal model. The reductions of parasite burden in macrophages (U937) and in hamsters have been described in supplementary information.

DIM induces apoptosis in leishmanial cells.

Induction of apoptosis causes the externalization of phosphatidyl serine on the surface of apoptotic cells (Sen et al., 2004a), which was detected by using annexin-V that binds with exposed phosphatidyl serine of apoptotic cells in a Ca^{2+}-dependent manner. Externalization of phosphatidyl serine was observed by confocal microscopy after treatment of promastigotes with

15 μM of DIM for 4 and 6 h (Fig. 2A). Treatment of promastigote cells with 10 μM protease inhibitor (VAD-fmk) causes disappearance of green rings around the cell membrane. This observation supports that the appearance of phosphatidyl serine on outer leaflet apparently requires caspase-like protease activation in *Leishmania* promastigote cells.

To determine the percentage of apoptotic and necrotic cells in *Leishmania* promastigotes, cells were incubated with DIM (15 μM) for 2, 4 and 6 h, and the percentages of cells undergoing apoptosis/necrosis were determined by flow cytometric analysis after staining with annexin V-FITC and PI (Fig. 2B). The cells in the lower right quadrant indicated apoptosis while in the upper right one represented post-apoptotic necrotic population. It is known that dead cells are reactive to PI and that externalized phosphatidylserine residues undergoing apoptosis are detected by annexin V-FITC. Flow cytometric analysis with annexin-V/PI staining showed that when cells were exposed to DIM (15 μM) for 2, 4 and 6 h, the percentage of apoptotic cells were increased with slight increase of necrotic cells. The proportion of apoptotic and necrotic cells increased from 3% and 1% in control cells to 34% and 4% respectively after treatment with DIM for 2 h. After 6 h of treatment, the proportion of apoptotic and necrotic cells were increased to 84% and 14%, respectively (Fig. 2C). The number of viable cells decreased from 96% to 12% after treatment with DIM for 6 h. Consistent with Figure 1A, 84% of *L.donovani* promastigotes show PCD after treatment with 15 μM of DIM for 6 h (Fig. 2B and C). These results suggest that DIM-induced apoptosis is the main cause of death.

DIM induces the formation of ROS inside the cells, which causes cellular oxidative stress.

Normally during oxidative phosphorylation the release of ROS in the form of superoxide anion occurs to the extent of 3% to 5% of total oxygen consumed (Boonstra et al., 2004). However,

under certain conditions when drugs inhibit oxidative phosphorylation, this rate of ROS production can be increased greatly (Mattiazzi et al., 2004). To determine whether the DIM functions in a similar manner, we examined the role of mitochondria in DIM-induced oxidative burst. Freshly prepared leishmanial mitochondria were treated separately with DIM at 15 µM, oligomycin at 10 µM and antioxidant NAC at 20 mM. DIM generates almost the same level of ROS as does oligomycin, a mitochondrial complex V inhibitor (Fig. 3A). It was also reported that the treatment with oligomycin A causes loss of mitochondrial membrane potential and increase in ROS production (Tettamanti et al., 2008). The mitochondrial ROS production is inhibited when cells were treated with NAC for different time periods and subsequently washed prior to the treatment with DIM. The results indicate that DIM has effects similar to oligomycin with respect to ROS generation in leishmanial cells. Therefore, the above results suggest that DIM-induced mitochondrial ROS generation is due to mitochondrial dysfunction, especially inhibition of respiratory chain. We have also measured the cytosolic ROS (Fig. 3A, Inset) and found that cytosolic ROS started to generate after 45 min of DIM treatment.

To further verify the effect of DIM on intracellular ROS levels, we treated leishmanial cells separately with DIM (15 µM), CPT (5 µM) and several antioxidants and examined the ROS production over time. Cellular ROS generated after treatment with DIM in *L.donovani* promastigotes, are measured fluorimetrically by conversion of H_2DCFDA to highly fluorescent 2,7-dichlorofluorescein. The level of peroxide radicals increased in parasites significantly within 1 h of treatment with DIM. When cells were treated with NAC, SB or mannitol before the treatment with DIM (15 µM), the level of ROS generation decreased. (Fig. 3B). From the above results it appears that the level of total cellular ROS generation remains same as that of mitochondrial ROS generation after 30 min of DIM treatment, whereas cytosolic ROS appears to

increase after 45 min. Therefore, it can be concluded that the level of total cellular ROS at 30 min is primarily contributed by the mitochondria and mitochondrial ROS generation preceeds cytosolic ROS generation.

DIM-induced oxidative stress causes depletion of the GSH level and increases the level of lipid peroxidation.

One of the most important cellular defences against intracellular oxidative stress is GSH, which plays a critical role in mediating apoptosis in eukaryotes including leishmanial cells. A decrease in GSH level causes an increase in the number of DIM-mediated DNA-protein cross-links. The actual mechanism by which GSH exerts its influence in leishmanial cells is yet to be explored. GSH is an important molecule for protecting kinetoplastids from ROS or toxic compounds and may induce a loss of $\Delta\Psi m$. DIM causes 40% decrease in GSH level after 2 h and the effect was more pronounced after 4 h of treatment with DIM. This inhibition is comparable with oligomycin treatment as shown in Fig. 4A. When cells were pre-incubated with NAC, before treatment with DIM, the decrease in GSH level was protected significantly and the level tends to become normal.

Lipid peroxidation is assessed by measuring total fluorescent lipid peroxidation products in leishmanial cells after treatment with DIM. The treatment leads to an increase in lipid peroxides after 2 h and reached to saturating level after 4 h. Oligomycin increases exactly the same level of lipid peroxidation as does DIM. When leishmanial cells were treated with butylated hydroxy toluene (BHT, 20 mM), a specific inhibitor of lipid peroxidation, and subsequently washed and then treated with DIM the level of fluorescent products decreased as observed in case of treatment with NAC at 20 mM (Fig. 4B). The above results suggest that the

effect of DIM is similar to the effect of oligomycin with respect to depletion of GSH level and increase the level of lipid peroxidation in leishmanial cells.

DIM inhibits mitochondrial FoF1-ATP synthase in leishmanial cells.

Since mitochondrial ROS production started earlier than cytosolic ROS and this ROS production was almost similar to oligomycin induced ROS production, so this mitochondrial ROS generation might be due to inhibition of complex V of electron transport chain (ETC). Mitochondrial respiration occurs via ETC containing five respiratory complexes located in the inner mitochondrial membrane. The FoF1-ATP synthase, a complex V of respiratory chain, is responsible for oxidative phosphorylation, which is the last step of ETC. Mitochondrial FoF1-ATP synthase (FoF1-ATPase) can catalyze both ATP synthesis and ATP hydrolysis. When there is a proton gradient, the enzyme catalyzes the forward reaction (ATP synthesis), and when there is no gradient, it displays FoF1-ATPase activity (Boyer, 1997).

In this study, we have shown that DIM inhibits the activity of mitochondrial FoF1-ATP synthase with IC_{50} of 8.75 μM, which was determined using 1% digitonin-solubilized freshly isolated mitochondria from *L. donovani* promastigotes. The result is summarized in Figure 5. DIM inhibits FoF1-ATP synthase activity in mitochondrial extract of *L. donovani* in a concentration dependent manner. FoF1-ATP synthase activity decreased to 9% at 1 μM DIM, whereas activity decreased significantly to 83% at 15 μM DIM in comparison to control ($p< 0.001$). Indole 3-carbinol (I3C), the precursor of DIM in plants, showed no effect on enzyme activity. The extent of inhibition by DIM at 20 μM is comparable with the effect of the well-known FoF1-ATP synthase inhibitor, oligomycin at 10 μM. Ouabain, a selective Na^+-K^+-ATPase

Molecular Pharmacology Fast Forward. Published on August 14, 2008 as DOI: 10.1124/mol.108.050161
This article has not been copyedited and formatted. The final version may differ from this version.

inhibitor has no effect on the total FoF1-ATP synthase activity, indicating that Na^+-K^+-ATPase activity does not interfere in this reaction.

As DIM inhibits mitochondrial FoF1-ATP synthase, a respiratory chain complex V, it might also interact with other complexes of the mitochondrial respiratory chain. In order to sort out this, we carried out the activity assay for other complexes with DIM. Spectrophotometric analysis (Table 1) of the activities of the complexes after treatment with DIM at 15 μM for 30 min revealed no such decrease in the activity of complex I, II, III and IV compared to the activity in the untreated control parasites. The treatment of DIM drastically reduces the activity of complex V to 17% at 30 min, which is comparable to the effect of oligomycin. This activity of complex V was further decreased to 10% after treatment with DIM for 120 min. Although there was no decrease of complex I activity at 30 min there was a modest decrease (23%) of activity at 120 min. Our experimental data shown that DIM is an inhibitor of ETC like oligomycin. To investigate the sensitivity of different ETC inhibitors on healthy growing respiring leishmanial cells, were treated with rotenone (complex I inhibitor), TTFA (complex II), antimycin A (complex III inhibitor), cyanide (complex IV inhibitor), and oligomycin (complex V inhibitor) separately. It was observed that each of these inhibitors could inhibit the activity of their respective complexes within 30 min of inhibition (Table 1).

DIM decreases cellular ATP levels in leishmanial cells.

DIM-mediated mitochondrial FoF1-ATP synthase inhibition was further confirmed by determination of cellular ATP levels. Treatment of *L.donovani* promastigote cells with DIM at 15 μM decreased the mitochondrial ATP level in a time dependent manner. The level of mitochondrial ATP had dropped by 30% at 15 min and 70% at 60 min after treatment with DIM.

Treatment with oligomycin A for the same period caused further decreased in ATP level upto 40% and 75% respectively. 2-Deoxy-D-glucose (5 mM), a glycolytic pathway competitive inhibitor has no effect on mitochondrial ATP level, even after 60 min of treatment (Fig. 6A).

In DIM-treated leishmanial cells, disruption in the function of mitochondria caused reduced ATP generation. Intracellular ATP is generated through both mitochondrial and glycolysis sources. 75% of total intracellular ATP is supplied by mitochondria and about 30% is contributed by glycolysis in leishmanial cells (Sen et. al., 2006). Here we have measured the cytosolic ATP level in differently treated cells (Fig. 6B). There was a gradual fall of ATP level to the extent of 45% after 2 h of treatment with DIM at 15 μM and to the extent of 58% after 2 h of treatment with 2-Deoxy-D-glucose (5 mM). ATP is the major readily useable form of energy involved in many crucial cellular processes. Because the glycolytic pathway and mitochondrial oxidative phosphorylation are the two major cellular ATP-generating pathways, we also measured the effect of co-treatment with DIM and 2-Deoxy-D-glucose on cellular ATP levels. Treatment with DIM prior to the treatment with 2-Deoxy-D-glucose further decrease cytosolic ATP level to the extent of 65%. The above results indicated that DIM-induced depletion of mitochondrial and cytosolic ATP levels are due to inhibition of mitochondrial oxidative phosphorylation.

DIM induces depolarization of mitochondrial membrane potential.

Depolarization of mitochondrial membrane potential ($\Delta\Psi m$) is a characteristic feature of apoptosis. To investigate weather $\Delta\Psi m$ decreases in DIM treated cells during apoptosis, a time-course study of $\Delta\Psi m$ was performed with DIM (Fig. 7A). $\Delta\Psi m$ was measured by spectrofluorimetric analysis with the mitochondrial membrane potential sensitive dye JC1, which

Molecular Pharmacology Fast Forward. Published on August 14, 2008 as DOI: 10.1124/mol.108.050161
This article has not been copyedited and formatted. The final version may differ from this version.

MOL # 50161

is a cationic dye that aggregates in the mitochondria of healthy cells. This aggregates fluoresce red at higher potential but at lower potential this reagent cannot accumulate in the mitochondria and remains as monomers in the cytoplasm. The monomeric dye fluoresces green that can be detected by a shift in fluorescence from red to green indicating the depolarization of mitochondrial membrane potential. The uptake of this dye by the mitochondria decreases with an increase in green fluorescence intensity in the cytosol. The sensitivity of JC1 dye to the change in mitochondrial membrane potential was determined by treating leishmanial cells with mitochondrial uncoupling agent carbonyl cyanide m-chloro-phenylhydrazone (CCCP, 1μM) that causes total depolarization of mitochondrial membrane potential. When cells were treated with antioxidants like N-acetyl-L-cysteine (NAC, 20 mM), sodium benzoate (SB, 20 mM), and mannitol (20 mM) or with lipid peroxidation inhibitor (BHT, 20 mM) before treatment with DIM (15 μM), loss of $\Delta\Psi m$ is prevented. This was evidenced from the mean green fluorescence intensity that is almost same as DMSO treatment and was also confirmed by the ratio of fluorescence intensity (590:530) represented in Figure 7B. The ratio between red (590 nm) and green (530 nm) signals is a measure of $\Delta\Psi m$. There is a significant increase (82%) in mean green fluorescence intensity within first 45 min of treatment with DIM as compared with relative $\Delta\Psi m$ observed after treatment with CCCP. The loss of $\Delta\Psi m$ continues to the extent of 91% after treatment with DIM for 60 min. However, treatment with CED3/CPP32 group of protease inhibitor (VAD-fmk) prior to the treatment with DIM for 60 min prevents the loss of mitochondrial membrane potential only to the extent of 74%. The above results indicate that mitochondrial ROS generation is responsible for the mitochondrial membrane depolarization and it is not due to caspase-like proteases.

To investigate weather FoF1-ATP synthase in leishmanial cells is involved in the depolarization of the mitochondrial membrane, we have performed an experiment in the presence of oligomycin (10 µM), an FoF1-ATP synthase inhibitor. It was observed that the mean green fluorescence intensity increases in oligomycin-treated cells. But when cells were treated with oligomycin (10 µM) and further incubated with DIM (15 µM), the effect on mitochondrial membrane depolarization is almost same as with oligomycin treatment alone (Fig. 7C). The above results suggest that inhibition of FoF1-ATP synthase is responsible for depolarization of mitochondrial membrane potential.

Loss of mitochondrial membrane potential causes release of cytochrome c.

The permeabilization of mitochondrial membrane causes the release of proapoptotic proteins including cytochrome c into the cytosol (Kluck et al., 1997). Cytochrome c, a component of the mitochondrial electron transport chain (ETC), is present in the inter-membrane space. Disruption of the outer mitochondrial membrane by apoptotic stimuli results in the release of cytochrome c into the cytosol where it initiates activation of caspase-like proteases leading to apoptosis. We have shown by western blotting that treatment with DIM causes cytochrome c accumulation in the cytoplasm of *Leishmania* (Fig. 8A, lanes 3 and 4). When cells were treated separately with antioxidants like NAC (20 mM), SB (20 mM) and mannitol (20 mM) for 1 h prior to the treatment with DIM (15 µM) for 6 h, the cytochrome c release into the cytosol is prevented (lanes 5-7). The results prove that mitochondrial ROS is responsible for the release of cytochrome c from mitochondria to cytosol. To investigate the role of CED3/CPP32 group of protease inhibitors in the release of cytochrome c in the cytosol, the cells were treated with VAD-fmk before treatment with DIM (lane 8). The result shows that these groups of protease

inhibitors do not affect the cytochrome c release into the cytosol. As control we have checked the presence of β-tubulin (a constitutive cytosolic protein) in the cytosol of *L.donovani* promastigotes treated with or without DIM.

DIM causes activation of caspase-like proteases in cytosol and cleavage of PARP protein.

The release of cytochrome c from mitochondria into the cytosol leads to an activation of the caspase cascade (Kupchan et al., 1969) and is a critical step in the activation of different caspases like caspase 9 and 3 which trigger the downstream events leading to apoptosis (Zou et al., 1997). Caspase 9 is a member of the ICE family of proteases and caspase 3 is a member of CED3/CPP32 group of proteases. To further substantiate the existence of these proteases in *L.donovani*, we carried out fluorometric assay of both ICE and CED3/CPP32 family of proteases using their specific substrates Leu-Glu-His-Asp-7-amino-4-methyl coumarin (LEHD-AMC) and Asp-Glu-Val-Asp-7-amino-4-trifluoromethyl coumarin (DEVD-AFC), respectively. The activities were measured in terms of liberation of AMC and AFC from their substrates. A significant increase in the activity of ICE group of proteases was observed after treatment with DIM for 4 h compared to 0.2% DMSO-treated control cells (Fig. 8B). A similar increase in the activity of CED3/CPP32 group of proteases were also observed after 4 h treatment with DIM (Fig. 8C). In the presence of specific inhibitor of these proteases (LEHD-CHO for ICE group and DEVD-CHO for CED3/CPP32 group), activities of these enzymes were inhibited.

PARP [poly (ADP ribose) polymerase], an enzyme involved in DNA repair, is a preferential substrate for caspase 3 (Tewari et al., 1995). We have determined the extent of PARP cleavage by immunoblot analysis of the PARP cleavage products (Fig. 8D). PARP protein (78 kDa) generates a 63 kDa cleaved fragment upon treatment of cells with DIM for 4 and 6 h,

where extent of PARP cleavage is more in 6 h. However, the cleavage of this PARP protein did not occur when cells were pretreated with VAD-fmk, a CED3/CPP32 group of protease inhibitor.

DIM induces the fragmentation of genomic DNA.

The inter-nucleosomal DNA digestion by an endogenous nuclease (genomic DNA fragmentation) is considered as a hallmark of apoptotic cell death (Compton, 1992). To establish the DIM-induced DNA fragmentation, we performed the DNA fragmentation assay by ELISA as described in Materials and Methods. It was observed that there was 56% and 73% fragmentation of DNA by treatment with DIM (15 µM) at 4 and 6 h respectively (Fig. 9A). The drug concentration (15 µM) used has been optimized on the basis of percentage of DNA fragmentation induced at 6 h of drug treatment. Further treatment with the drug for 8 h did not increase DNA fragmentation and it remains almost same as before (78%). Treatment with protease inhibitor VAD-fmk and antioxidant NAC for 6 h reduced the percentage of DNA fragmentation to 42% and 37% respectively. So these results indicate that both caspase-like protease and ROS are also responsible for DNA fragmentation in DIM-induced cell death.

DIM arrests cell cycle progression at G_1-phase in *L. donovani* promastigote cells.

The cell cycle distribution was analyzed by flow cytometry following treatment with DIM for different time periods (Fig. 9B). In control cells the G_1, S and G_2-M population remain almost same throughout the experiment. DIM caused *L.donovani* promastigotes to remain at resting G_0/G_1 phase and inhibits their entry into the S phase. The flow cytometric experiment shows that

Molecular Pharmacology Fast Forward. Published on August 14, 2008 as DOI: 10.1124/mol.108.050161
This article has not been copyedited and formatted. The final version may differ from this version.

84% of cells are in G_1 phase, whereas 12% are in S phase and 4% in G_2/M phase after treatment with DIM at 15 μM for 6 h.

DIM inhibits DNA synthesis in *Leishmania* promastigotes.

The effect of DIM on DNA synthesis was studied by the incorporation of [^{3}H] thymidine into DNA of *L.donovani* promastigotes in presence and in absence of different concentrations of DIM (Fig. 9C). Incubation for 12 hours with 10, 20, 50 and 100 μM DIM decreases [^{3}H] thymidine incorporation to 49%, 32%, 14% and 7% respectively. After 24 h of incubation with DIM at the above concentrations, the incorporation decreased to 46%, 23%, 11% and 6% respectively. The decreases in the rate of thymidine incorporation with time at a particular concentration indicate a decrease in DNA replication activity within parasites. Taken together, the results suggest that DIM is very effective in inhibiting DNA synthesis

Mitochondrial DNA depleted leishmanial cells (mtDDC) do not undergo DIM-induced PCD.

To investigate whether DIM can induce PCD in mitochondrial DNA depleted leishmanial cells (mtDDC), we have developed dyskinetoplastid parasites by treatment with berenil (20 μM) for 24 h (Sen et al., 2004a). We have performed the assay for respiratory complexes activity (Table 2) and also confocal microscopic experiment (Supplementary Fig. S2) in mtDDC to characterize the depletion of mt-DNA in the parasites. It was observed that all the complexes except complex II lose their activities in mtDDC). This is because the components of only complex II are encoded in genomic DNA and the components of other complexes are encoded in the genomic DNA as well as mitochondrial DNA. Therefore, only complex II activity remains same in

mtDDC as in wild type *Leishmania* parasites. The cells were washed and suspended in berenil-free media and supplemented with pyruvate and uridine. In another set of experiments after berenil treatment the cells were washed and suspended in berenil-free growth media without pyruvate and uridine. Mitochondrial DNA depleted cells can only grow in the presence of pyruvate and uridine, but the doubling time of these auxotrophic cells increased compared to normal healthy cells (Sen et al., 2007b). In both cases cells were allowed to grow in presence of 0.2% DMSO and 15 μM DIM separately for different time periods and the viable parasites were measured by MTT assay. We have shown that only 25% growth was inhibited by 15 μM DIM at 8 h in mitochondrial DNA depleted leishmanial cells, whereas 95% growth was inhibited by same concentration of DIM at same time period in wild-type healthy parasites (Fig. 10A). We have also found that this 25% growth inhibition was not due to apoptosis as these cells do not respond to staining with Annexin-V (data not shown). The inhibition of growth might be due to delayed nonapoptotic death in presence of DIM that is a consequence of prolonged loss of mitochondrial function. This result is consistent with other studies where it was shown that delayed nonapoptotic death occurred in presence of caspase inhibitors in neuronal cells (Stefanis et al., 1999). We have also shown that in mt-DNA depleted cells intracellular ATP production decreased to 0.5 nmol ATP/10^7 cells (Fig. 10B). When these cells were allowed to grow in a media supplemented with pyruvate and uridine intracellular ATP level increased to 1.2 nmol ATP/10^7 cells in absence of DIM at 16 h. This result is consistent with previous report (Sen et al., 2007b). The intracellular ATP level increased to 1.17 nmol ATP/10^7 cells in presence of 15 μM DIM at 16 h, which is almost same level of intracellular ATP in absence of DIM. Mitochondrial DNA depleted leishmanial cells can maintain glycolytic process and continue to survive only in the presence of pyruvate and uridine (Sen et al., 2007b). Therefore, the above

results suggest that mt-DNA depleted leishmanial cells are insensitive to DIM and DIM-induced PCD occurred through mitochondria dependent cascade machinery.

To investigate the possible reasons, we have measured mitochondrial ROS level. It was observed that when mt-DNA depleted cells were treated with DIM these auxotrophic cells were unable to produce ROS inside cells (Fig. 10C). This was further evidenced from the observation that mitochondrial membrane potential (Fig. 10D) also remains unaltered in these auxotrophic cells unlike normal cells after treatment with DIM for 1 h. Moreover, unlike healthy cells no apoptotic phenomenon like DNA fragmentation was observed during treatment with DIM to these auxotrophic cells (data not shown). As the formation of ROS is exclusively needed for the initiation and propagation of DIM-induced PCD in leishmanial cells, it can be assumed that inhibition of ROS formation prevents the cells to undergo apoptosis. But the question remains that why the dyskinetoplastid cells were unable to produce ROS even in the presence of DIM. The major source of ROS production inside cells is the mitochondria irrespective of higher or lower eukaryotes. Any mutation or dysfunction within the mitochondria will block the electron transfer within or between mitochondrial respiratory complexes and causes leakage of electrons (Wei et al., 2001). Mitochondrial dysfunction is most likely an adaptive process to the over production of ROS inside cells. From our previous study it was observed that topoisomerases are present both in mitochondria and in the nucleus (Das et al., 2004). DIM, a potent anti-tumor agent can trap topoisomerase I mediated cleavable complexes (Roy et al., 2008). Stabilization of these complexes inside mitochondria decreases cellular oxygen consumption and facilitates the generation of ROS in healthy cells. Here in the case of mtDDC, treatment with DIM was unable to form cleavable complex and subsequently fails to generate ROS inside cells. These may be the probable mechanism for the insensitiveness of the dyskinetoplastid cells to DIM. Moreover,

leishmanial cells have only one giant mitochondrion unlike higher eukaryotes. So in the absence of the mitochondrial DNA, these mt-DNA depleted cells can not induce the formation of toxic ROS inside cells even in the presence of DIM. However, it should be mentioned that the presence of pyruvate and uridine in the growth media does not inhibit the ROS production during treatment with DIM in healthy cells. Collectively, DIM-induced PCD is inhibited in mtDDC unlike higher eukaryotic cells and this might be a useful model for understanding the mechanism of DIM-induced PCD in *Leishmania* parasites.

Molecular Pharmacology Fast Forward. Published on August 14, 2008 as DOI: 10.1124/mol.108.050161
This article has not been copyedited and formatted. The final version may differ from this version.

Discussion:

Recently, we have shown that DIM directly stabilizes the formation of topoisomerase I-DNA cleavable complexes in leishmanial cells and acts as a topoisomerase I poison like CPT (Roy et al., 2008). Topoisomerase I is present both in mitochondria and nucleus. CPT, a potent anti-tumour agent can trap topoisomerase I mediated cleavable complex in the mitochondria (Bodley and Shapiro, 1995) and increases the cellular ROS generation in leishmanial cells (Sen et al., 2004a). Since DIM stabilizes the topo I-DNA cleavable complexes like CPT, it might generate ROS inside mitochondria. Therefore, we have measured the endogenous ROS in leishmanial cells after treatment with DIM. It was found that there is consistent increase in mitochondrial ROS. One of the causes of mitochondrial ROS generation is dysfunction of mitochondrial respiratory chain (Mehta A and Shaha C, 2004).

DIM-induced topo I-DNA covalent complex formation generates reactive oxygen species (ROS) inside cells (Sen et al., 2004a). This event cannot explain the accumulation of huge amount of ROS inside the mitochondria and rapid onset of the death process. Therefore, we speculate that some mitochondrial dysfunction is invariably involved in initiating the apoptotic process. Dysfunction of mitochondrial respiratory chain can produce the huge amount of ROS inside the mitochondria. Recently, DIM has been reported to inhibit mitochondrial H^+-ATP synthase and induce apoptosis in human breast cancer cells (Gong et al., 2006). Moreover, presence of an oligomycin-sensitive FoF1-ATP synthase responsible for oxidative phosphorylation has already been demonstrated in leishmanial cells (Sen et al., 2004a). We therefore checked the effect of treatment of DIM on respiratory chain complexes in mitochondria isolated from *L.donovani* cells. DIM was found to severely inhibit the complex V activity, which comprises of the FoF1-ATP synthase. Identification of the mitochondial target led us to further

investigate the role of mitochondria and the downstream events in leishmanial cells undergoing PCD following DIM treatment.

Mitochondria are the principal site for the generation of cellular ATP by oxidative phosphorylation. Given the importance of mitochondria for cell life, it comes as no surprise that mitochondrial dysfunction and failure leads to cell death. So mitochondria are the main target of injury after stresses leading to programmed cell death and necrosis. As in most eukaryotes, in kinetoplastids the mitochondrion is also responsible for the cellular respiration and phosphorylation processes. Mitochondrial respiration occurs via electron transport chain (ETC) containing five respiratory complexes located in the inner mitochondrial membrane. The FoF1-ATP synthase, a complex V of respiratory chain, is responsible for oxidative phosphorylation, which is the last step of ETC. The FoF1-ATP synthase in *Leishmania* parasites consists of two oligomeric components Fo and F1. Fo is an integral membrane protein that contains the proton channel and comprises some subunits encoded by nuclear DNA and two subunits encoded by mt-DNA. F1 is a peripheral membrane protein that contains the ATP synthase active sites and made up of five subunits ($\alpha_3\beta_3\gamma\delta\varepsilon$). In leishmanial cells ATP synthesis requires the involvement of both Fo and F1 components. This F-type ATP synthase is ubiquitously located in the inner membrane of the mitochondria and is responsible for the synthesis of ATP in the oxidative phosphorylation pathway (Kupchan et al., 1969). The role of this protein for depolarization of mitochondrial membrane potential has been reported previously in leishmanial cells (Sen et al., 2004a). Mitochondrial membrane depolarization is dependent on the utilization of glycolytic ATP by oligomycin-sensitive FoF1-ATP synthase in the reverse mode. In case of *Leishmania* parasites, mitochondrial depolarization occurs before the increase in the number of apoptotic cells. This event proves that depolarization of mitochondrial membrane potential is a pre-

apoptotic event, which is an irreversible commitment of the cell to PCD after administration of DIM. We have shown that mitochondrial depolarization is enhanced after treatment with DIM similar to that with oligomycin. Therefore, it can be concluded that FoF1-ATP synthase in *Leishmania* plays a very important role in depolarization of mitochondrial membrane potential ($\Delta\Psi m$).

There was depletion of mitochondrial ATP level in DIM treated cells and the extent of depletion within 15 min was almost 30%. This depletion of mitochondrial ATP level reduced by 70% after 1 h treatment with DIM, whereas 2-Deoxy-D-g1ucose has no significant effect on mitochondrial ATP level. Almost same extent of mitochondrial ATP depletion was observed in oligomycin-treated cells. The above results suggest that mitochondrial ATP depletion after treatment with DIM is due to inhibition of mitochondrial oxidative phosphorylation. Concerning the cellular bio-energy of the leishmanial cells in PCD, it is observed that the cellular ATP level gradually decreases as opposed to mammalian cells. This might be due to the fact that in higher eukaryotes not all mitochondria are responsible for cytochrome c release and that a portion maintains their trans membrane potential and supply ATP to continue the apoptosis. Thus it appears that the healthy mitochondria ensure compensation for the injured ones in mammalian cells after induction of apoptosis. But for organisms with single mitochondrion like *L.donovani*, there is no possibility for the compensation of injured mitochondria and survival depends on proper functioning of a single organelle. In the absence of proper functional mitochondria, cells would cease to synthesize ATP from their mitochondrial source and cause a rapid decrease in cellular ATP levels to the extent of 70% by 60 min. Our result is consistent with the study reported earlier that the ATP level gradually decreases after the loss of $\Delta\Psi m$ during treatment with H_2O_2 (Mukherjee et al., 2002). But ATP is a key molecule for chromatin condensation,

nuclear fragmentation and regulation, and maintenance of ion homeostasis during apoptosis. So we can assume that the ATP levels generated before the loss of ΔΨm and ATP supplied by glycolysis are sufficient to carry out these cellular activities and to propagate PCD in leishmanial cells.

The depolarization of ΔΨm is due to inhibition of FoF1-ATP synthase activity, depletion of ATP and generation of oxidative stress (ROS), which leads to the release of cytochrome c from mitochondria into cytosol and activates caspase-like proteases. There are evidences that the caspase-like proteases play important roles in the apoptotic cascade of unicellular kinetoplastid parasites after induction of different stimuli (Das et al., 2001; Lee et al., 2002). Although metacaspases (Moss et al., 2007) and some nucleases like endonuclease G (Gannavaram et al., 2008) are known to be activated through apoptotic cascade in unicellular protozoan parasites, the activation of CED3/CPP32 group of proteases and ICE family of proteases are well established in leishmanial cells (Sen et al., 2004a; Sen et al., 2004b; Sen et al., 2007; Das et al., 2001). Therefore, the possibility of the presence of caspase-like proteases in leishmanial cells cannot be ruled out. In the present study, we have shown that ICE family of proteases were activated before the activation of CED3/CPP32 group of proteases in leishmanial cells, following DIM treatment. In the presence of CED3/CPP32 group of protease inhibitor (VAD-fmk), downstream events of caspase 3-like protease activation such as PARP cleavage and DNA fragmentation were prevented, which suggest that the CED3/CPP32 group of proteases are involved in DIM-induced PCD of leishmanial cells.

Finally, we have checked the effects of DIM on mtDDC to investigate the role of mitochondria in DIM-induced PCD. It was found that mtDDC are insensitive to DIM and failed to generate mitochondrial ROS and ATP depletion. Moreover, unlike healthy cells no apoptotic

phenomenon like DNA fragmentation was observed during treatment with DIM to these auxotrophic cells. Therefore, the above results strongly support the mitochondria dependent and ROS-mediated DIM-induced PCD in leishmanial cells.

In conclusion, our study demonstrates for the first time that DIM inhibits mitochondrial FoF1-ATP synthase and induces PCD in kinetoplastid parasites. The inhibition of FoF1-ATP synthase by DIM likely represents an essential event responsible for the propagation of PCD and can act as a central regulator of the apoptotic machineries. Moreover, it is worth mentioning that formation of topoisomerase I-DNA suicidal complexes is responsible for DNA fragmentation and is necessary to amplify the apoptotic process (Lee et al., 2002). Our study identified a further important mode of action for the intriguing dietary component DIM that induces mitochondria dependent PCD as the effects seen from treatment with DIM are a consequence of its inhibition of the mitochondrial FoF1-ATP synthase in protozoan parasite *L.donovani*. The upstream events of generation of ROS are different from other mechanistic pathways induced by DIM in different cell lines (Xue et al., 2008). Mitochondrial membrane depolarization and ROS formation play significant roles in modulating the response of the parasite to DIM. The mitochondrial DNA depleted leishmanial cells do not undergo PCD after treatment with DIM. The occurrence of these molecular events provide substantial evidences in support of the fact that the PCD machinery in unicellular organisms like kinetoplastids may have evolved through a process of horizontal gene transfer or evolutionary convergence. So understanding the molecular mechanism of the cascade of programmed cell death (Fig. 11) provides the opportunities for discovering and evaluating molecular targets for drug designing that might be exploited for the therapeutic development against human leishmaniasis.

Molecular Pharmacology Fast Forward. Published on August 14, 2008 as DOI: 10.1124/mol.108.050161
This article has not been copyedited and formatted. The final version may differ from this version.

Acknowledgement:

We thank Prof. S. Roy, the Director of Indian Institute of Chemical Biology (IICB), Kolkata, India, for his interest in this work.

References:

Bodley AL and Shapiro TA. (1995) Molecular and cytotoxic effects of camptothecin, a topoisomerase I inhibitor, on trypanosomes and Leishmania. *Proc Natl Acad Sci U S A.* **92:** 3726-3730.

Boyer PD. (1997) The ATP synthase--a splendid molecular machine. *Annu Rev Biochem.* **66:** 717-749.

Boonstra J and Post JA. (2004) Molecular events associated with reactive oxygen species and cell cycle progression in mammalian cells. *Gene.* **337:** 1-13.

Chowdhury, A.R., Sharma, S., MandaI, S., Goswami, A., Mukhopadhyay, S. and Majumder, H.K. (2002) Luteolin, an emerging anti-cancer flavonoid, poisons eukaryotic DNA topoisomerase I. *Biochem. J.* **366:** 653-661.

Compton MM. (1992) A biochemical hallmark of apoptosis: internucleosomal degradation of the genome. *Cancer Metastasis Rev.* **11:** 105-119.

Das M, Mukherjee SB. and Shaha C. (2001) Hydrogen peroxide induces apoptosis-like death in *Leishmania donovani* promastigotes. *J Cell Sci.* **114**: 2461-9.

Facompre M, Goossens JF, Bailly C. (2001) Apoptotic response of HL-60 human leukemia cells to the antitumor drug NB-506, a glycosylated indolocarbazole inhibitor of topoisomerase 1. *Biochem Pharmacol.* **61:** 299-310.

Gannavaram S, Vedvyas C, Debrabant A. (2008) Conservation of the pro-apoptotic nuclease activity of endonuclease G in unicellular trypanosomatid parasites. *J Cell Sci.* **121**: 99-109.

Green DR, Reed JC. (1998) Mitochondria and apoptosis. *Science.* **281**: 1309-1312.

Gong Y, Sohn H, Xue L, Firestone GL. and Bjeldanes LF. (2006) 3,3'-Diindolylmethane is a novel mitochondrial H (+)-ATP synthase inhibitor that can induce p21 (Cip1/Waf1) expression by induction of oxidative stress in human breast cancer cells. *Cancer Res.* **66**: 4880-7.

Gottlieb, R.A. (2001) Mitochondria and apoptosis. *Bioi Signals Recept.* **10:** 147-61.

Harris ME, Moore DR and Hajduk SL. (1990) Addition of uridines to edited RNAs in trypanosome mitochondria occurs independently of transcription. *J Bioi. Chem.* **265**: 11368-11376.

Hase Y, Tatsuno M, Nishi T, Kataoka K, Kabe Y, Yamaguchi Y, Ozawa N, Natori M, Handa H, Watanabe H. (2008) Atrazine binds to F1F0-ATP synthase and inhibits mitochondrial function in sperm. *Biochem. Biophys. Res Commun.***366**: 66-72.

Hong, C., Kim, H.A., Firestone, G.L. and Bjeldanes, L.F. (2002) 3,3'-Diindolylmethane (DIM) induces a G (1) cell cycle arrest in human breast cancer cells that is accompanied by Sp1-mediated activation of p21 (WAF1/CIP1) expression. *Carcinogenesis.* **23**: 1297-1305.

Halliwell B. and Gutteridge JM. (1990) Role of free radicals and catalytic metal ions in human disease: an overview. *Methods Enzymol.* **186**: 1-85.

Iwu MM, Jackson JE and Schuster BG. (1994) Medicinal plants in the fight against leishmaniasis. *Parasitol. Today.* **10**: 65-68.

Johnson TM, Yu ZX, Ferrans VJ, Lowenstein RA and Finkel T. (1996) Reactive oxygen species are downstream mediators of p53-dependent apoptosis. *Proc Natl Acad Sci USA.* **93:** 11848-11852.

Kluck RM, Bossy-Wetzel E, Green DR, Newmeyer DD. (1997) The release of cytochrome c from mitochondria: a primary site for Bcl-2 regulation of apoptosis. *Science.* **275:** 1132-36.

Lee N, Bertholet S, Debrabant A, Muller J, Duncan Rand Nakhasi HL. (2002) Programmed cell death in the unicellular protozoan parasite Leishmania. *Cell Death Differ*.**9:** 53-64.

Mattiazzi M, Vijayvergiya C, Gajewski CD, DeVivo DC, Lenaz G, Wiedmann M, Manfredi G. (2004) The mtDNA T8993G (NARP) mutation results in an impairment of oxidative phosphorylation that can be improved by antioxidants. *Hum Mol Genet.* **13:** 869-79.

Mehta A, Shaha C. (2004) Apoptotic death in *Leishmania donovani* promastigotes in response to respiratory chain inhibition: complex II inhibition results in increased pentamidine cytotoxicity. *J Biol Chem.* **279:**11798-813.

Mittra B, Saha A, Chowdhury AR, Pal C, Mandai S, Mukhopadhyay S, Bandyopadhyay S and Majumder HK. (2000) Luteolin, an abundant dietary component is a potent anti-leishmanial agent that acts by inducing topoisomerase II-mediated kinetoplast DNA cleavage leading to apoptosis. *Mol Med.* **6:** 527-541.

Mosman, T. (1983) Rapid Colorimetric assay for cellular growth and survival: application to proliferation and cytotoxic assays. *J Immuol. Methods.* **65:** 5-63.

Moss CX, Westrop GD, Juliano L, Coombs GH, Mottram JC. (2007) Metacaspase 2 of *Trypanosoma brucei* is a calcium-dependent cysteine peptidase active without processing. *FEBS Lett.* **581:** 5635-9.

Mukherjee SB, Das M, Sudhandiran G and Shaha C. (2002) Increase in cytosolic $Ca2^{+}$ levels through the activation of non-selective cation channels induced by oxidative stress causes mitochondrial depolarization leading to apoptosis-like death in *Leishmania donovani* promastigotes. *J Bioi. Chem.* **277:** 24717-27.

Rahman, K.W. and Sarkar, F.H. (2005) Inhibition of nuclear translocation of nuclear factor- {kappa} B contributes to 3,3'-diindolylmethane-induced apoptosis in breast cancer cells. *Cancer Res.* **65:** 364-371.

Roy A, Das BB, Ganguly A, Bose Dasgupta S, Khalkho NV, Pal C, Dey S, Giri VS, Jaisankar P, Dey Sand Majumder HK. (2008) An insight into the mechanism of inhibition of unusual bi-subunit topoisomerase I from *Leishmania donovani* by 3,3'-di-indolylmethane, a novel DNA topoisomerase I poison with a strong binding affinity to the enzyme. *Biochem J.* **409:** 611-622.

Salomon AR, Voehringer DW, Herzenberg LA, Khosla C (2001) Apoptolidin, a selective cytotoxic agent, is an inhibitor of F0F1-ATPase. *Chem Bioi.* **8:** 71-80.

Shapiro TA, Klein VA and Englund PT. (1989) Drug-promoted cleavage of kinetoplast DNA minicircles. Evidence for type II topoisomerase activity in trypanosome mitochondria. *J Bioi Chern.***264:** 4173-4178.

Sen N, Das BB, Ganguly A, Mukherjee T, Tripathi G, Bandyopadhyay S, Rakshit S, Sen T, Majumder HK. (2004a) Camptothecin induced mitochondrial dysfunction leading to programmed cell death in unicellular hemoflagellate Leishmania donovani. *Cell Death Differ.* **11:** 924-36.

Sen N, Das BB, Ganguly A, Mukherjee T, Bandyopadhyay S, Majumder HK. (2004b) Camptothecin-induced imbalance in intracellular cation homeostasis regulates

programmed cell death in unicellular hemoflagellate Leishmania donovani. *J Bioi Chem.***279:** 52366-75.

Sen N, Das BB, Ganguly A, Banerjee B, Sen T, Majumder HK. (2006) *Leishmania donovani*: intracellular ATP level regulates apoptosis-like death in luteolin induced dyskinetoplastid cells. *Exp Parasitoi.* **114:** 204-14.

Sen N, Banerjee B, Das BB, Ganguly A, Sen T, Pramanik S, Mukhopadhyay S, Majumder HK. (2007a) Apoptosis is induced in leishmanial cells by a novel protein kinase inhibitor withaferin A and is facilitated by apoptotic topoisomerase I-DNA complex. *Cell Death Differ.* **14:** 358-67.

Sen N, Banerjee B, Sen Gupta S, Das BB, Ganguly A, Majumder H K. (2007b) *Leishmania donovani*: Dyskinetoplastid cells survive and proliferate in the presence of pyruvate and uridine but do not undergo apoptosis after treatment with camptothecin. *Exp Parasitoi.* **115:** 215-19.

Stefanis L, Park DS, Friedman WJ, Greene LA. (1999) Caspase-dependent and -independent death of camptothecin-treated embryonic cortical neurons. *J Neurosci*. **19**: 6235-47.

Tettamanti G, Malagoli D, Ottaviani E, de Eguileor M. (2008) Oligomycin A and the IPLB-LdFB insect cell line: actin and mitochondrial responses. *Cell Bioi Int.* **32:** 287-92.

Tewari M, Quan LT, O'Rourke K, Desnoyers S, Zeng Z, Beidler DR, Poirier GG, Salvesen GS, Dixit VM. (1995) Yama/CPP32 beta, a mammalian homolog of CED-3, is a CrmA-inhibitable protease that cleaves the death substrate poly (ADP-ribose) polymerase. *Cell.* **81**: 801-809.

Vander Heiden MG, Chandel NS, Williamson EK, Schumacker PT and Thompson CB. (1997) Bcl-xL regulates the membrane potential and volume homeostasis of mitochondria. *Cell.* **91:** 627-637.

Xue L, Pestka JJ, Li M, Firestone GL, Bjeldanes LF. (2008) 3,3'-Diindolylmethane stimulates murine immune function in vitro and in vivo. *J Nutr Biochem.* **19**: 336-44

Zheng J, Ramirez YD. (1999) Piceatannol, a stilbene phytochemical, inhibits mitochondrial F0F1-ATPase activity by targeting the F1 complex. *BiochernBiophys Res Commun.* **261:** 499-503.

Zou H, Henzel WJ, Liu X, Lutschg A, and Wang X. (1997) Apaf-1, a human protein homologous to C. elegans CED-4, participates in cytochrome c-dependent activation of caspase-3. *Cell.* **90:** 405-413.

Footnotes:

This work was supported by the grants from Network Project NWP-38 of Council of Scientific and Industrial Research (CSIR), Government of India.

Molecular Pharmacology Fast Forward. Published on August 14, 2008 as DOI: 10.1124/mol.108.050161
This article has not been copyedited and formatted. The final version may differ from this version.

Legends for Figures:

Figure 1: Microscopic analysis of *in vitro* cytotoxicity of DIM. (**A**). Log phase promastigote cells (3 X 10^6) were cultured for 12 h in M199 media supplemented with 10% FBS and treated with 1, 5, 10, 15 and 20 µM of DIM for 2, 4, 8 and 12 h. Percentage of viable promastigotes was measured by MTT assay. (**B**). *L.major, L.tropica* and *L.tarentolae* promastigotes were also cultured in the presence of 15 µM DIM for 2, 4, 8 and 12 h. The percentage of viable promastigotes was measured by MTT assay. All data are expressed as percentage of live promastigotes and represent mean ± S.D. from three independent experiments. (**C**). Calculation of IC_{50} of amastigotes. U937 macrophages were allowed to adhere on cover slips on RPMI-1640 media supplemented with 10% FBS before in vitro infection with *L.donovani* AG83 promastigotes, followed by further incubation for 12 h at 37^0C with increasing concentrations of DIM (1, 5, 10 and 15 µM). The experiments were performed three times and representative data from one set of these experiments are expressed as mean ± SD.

Figure 2: Determination of downstream effects of caspase-like proteases in the presence of DIM and CED3/CPP32 group of protease inhibitor. (**A**). Externalization of phosphatidyl serine was detected in *L.donovani* promastigote cells. Annexin V labeling of *L.donovani* promastigotes was measured after treatment with 0.2% DMSO (1), with DIM (15 µM) for 4 h and 6 h (2 and 3), and with CED3/CPP32 group of protease inhibitor (VAD-fmk) prior to treatment with DIM (4). Pictures are representative of one of three similar results. (**B**). Apoptotic cells detected by flow cytometric analysis using annexinV and PI in FL-1 vs FL-2 channels. The cells were treated (I) without DIM, (II) with DIM (15 µM) for 2 h, (III) with DIM (15 µM) for 4 h and (IV) with DIM (15 µM)

for 6 h as described in Material and Methods. The cells in the lower right quadrant indicated apoptosis while in the upper right one represented post-apoptotic necrotic population. FACS data are representative one of three similar experiments. (**C**). Bar diagram showing the viable cells, apoptotic cells and necrotic cells as determined by FACS analysis. The results depicted were performed three times and representative data from one set of experiments are expressed as means ± SD. Variations among different set of experiments were <6%. ***p<0.001 compared to apoptotic cells with necrotic cells at 6 h.

Figure 3: Measurement of DIM-induced ROS generation. (**A**). Generation of peroxide radicals within the mitochondria was measured after treatment with 0.2% DMSO, DIM (15 µM), oligomycin (10 µM) and NAC (20 mM) treatment prior to the treatment with DIM. In inset, generation of peroxide radicals within the cytosol was measured after treatment with DMSO (0.2%) and DIM (15 µM) (**B**). Generation of intracellular peroxide radicals was measured after treatment with 0.2% DMSO, DIM (15 µM), CPT (5 µM), and with NAC, SB and mannitol separately prior to the treatment with DIM as described in Materials and Methods. The experiments were performed three times and representative data from one set of these experiments are expressed as mean ± SD.

Figure 4: Determination of intracellular GSH level and level of lipid peroxidation. (**A**). Level of intracellular GSH in treated and untreated *L.donovani* promastigotes. The intracellular GSH level was measured after treatment with 0.2% DMSO, CPT (5 µM), DIM (15 µM) and oligomycin (10 µM) separately and with NAC (20 mM) prior to treatment with DIM. Intracellular GSH level has been corrected and normalized according to the number of viable parasites. (**B**). The level of fluorescent products of lipid

peroxidation was measured after treatment of leishmanial cells with 0.2% DMSO, CPT (5 μM), DIM (15 μM), oligomycin (10 μM) and with NAC and BHT separately prior to treatment with DIM. The experiments were performed three times and representative data from one set of these experiments are expressed as mean ± SD.

Figure 5: 3,3'-Diindolymethane (DIM) inhibited mitochondrial FoF1-ATP synthase activity. DIM inhibited FoF1-ATPase activity in 1% digitonin-solubilized mitochondria isolated from *L.donovani* promastigote cells. The preparation of mitochondria and PK/LDH-coupled ATPase assay was described in Materials and Methods. ***p<0.001 compared to 15 μM DIM treatment with 1 μM DIM treatment.

Figure 6: Measurement of cellular ATP level. (**A**). DIM depletes mitochondrial ATP levels. Relative mitochondrial ATP level was determined at different times after treatment with 15 μM DIM, 10 μM oligomycin, 5 mM 2-deoxy-D-glucose and 15 μM DIM prior to treatment with 2-deoxy-D-glucose. (**B**). DIM depletes cytosolic ATP levels. Relative cytosolic ATP level was determined at different times after treatment with 15 μM DIM, 10 μM oligomycin, 5 mM 2-deoxy-D-glucose and 15 μM DIM treatment separately prior to treatment with 2-deoxy-D-glucose. Cellular ATP level has been corrected and normalized according to the number of viable parasites. The experiments were performed three times and representative data from one set of these experiments are expressed as mean ± SD.

Figure 7: Fluorimetric analysis of mitochondrial membrane potential (ΔΨm). (**A**). Changes of ΔΨm after treatment with 0.2% DMSO alone (control) and with DIM (15 μM), uncoupling agent CCCP (1 μM) as positive control, NAC (20 mM), SB (20 mM), mannitol (20 mM) as antioxidants, BHT (20 mM) as lipid peroxidation inhibitor, and

Molecular Pharmacology Fast Forward. Published on August 14, 2008 as DOI: 10.1124/mol.108.050161
This article has not been copyedited and formatted. The final version may differ from this version.

VAD-fmk (10 μM) as protease inhibitor prior to the treatment with DIM (15 μM) for 15, 30, 45 and 60 min respectively. (**B**). Ratio of fluorescence intensity was measured at 590/530, which was plotted at y-axis with different concentration of drugs after treatment for 60 min. ****p*<0.001 compared to DIM treatment alone with NAC plus DIM treatment. (**C**). Effects of treatments with CPT (5 μM) for 4 h as positive control, DIM (15 μM) for 0.5 h and 1 h, oligomycin (10 μM) for 1h and oligomycin prior to the treatment with DIM on the mitochondrial membrane potential of *L.donovani* promastigotes as measured by fluorescence of JC1 at 530 nm. The experiments were performed three times and representative data from one set of these experiments are expressed as mean ± SD. **p<0.01, ***p<0.001 compared to control. Mitochondrial membrane potential ($\Delta\Psi m$) has been corrected and normalized according to the number of viable parasites.

Figure 8: Determination of cytochrome c release, caspase-like proteases activity and PARP cleavage in *L.donovani* promastigotes. (**A**). Western blot analysis to detect the release of cytochrome c into the cytoplasm of differently treated cells. Lane 1, total level of cytochrome c in untreated leishmanial cells. Lane 2, control cells; lanes 3-4, cells treated with DIM (15 μM) for 4 and 6 h respectively. Lanes 5-8, treated with NAC, SB, BHT and VAD-fmk separately prior to treatment with DIM for 6 h. As loading control cytosolic fractions from differently treated cells were analyzed for the presence of β-tubulin by western blotting. (**B**). Activation of ICE group of proteases in the cytosol of leishmanial cells was measured after treatment with 0.2% DMSO, DIM (15 μM) and with LEHD-CHO inhibitor to DIM-treated cells as described in figure. (**C**). Activation of CED3/CPP32 group of proteases inside the leishmanial cells was measured after

treatment with 0.2% DMSO, DIM (15 μM) and with DEVD-CHO inhibitor to DIM-treated cells as described in figure. Results are mean ± SD. from three independent experiments. (**D**). Western blot analysis to detect the cleavage of full-length PARP protein after treatment with 0.2% DMSO (lane 1), with DIM (15 μM) for 4 h and 6 h (lanes 2-3), and with CED3/CPP32 group of protease inhibitor (VAD-fmk) prior to treatment with DIM (lane 4).

Figure 9: DIM-induced DNA fragmentation, cell cycle arrest and inhibition of DNA synthesis. (**A**). Relative percentage of DNA fragmentation measured by cell death detection ELISA kit in *L.donovani* promastigote cells treated with DIM (15 μM), with VAD-fmk and NAC separately prior to treatment with DIM and with VAD-fmk and NAC together prior to treatment with DIM at the concentrations mentioned above. The experiments were performed three times and representative data from one set of these experiments are expressed as mean ± SD. (**B**). DIM-mediated G_1 cell cycle arrest in *L.donovani* AG83 promastigote cells. Histograms of distribution of DNA content with flow cytometry in *Leishmania* cells. Cell cycle arrest was analyzed after treatment with 0.2% DMSO as control, and with DIM (15 μM) for 2 h, 4 h and 6 h. Cells were then stained with propidium iodide, and nuclei were analyzed for DNA content by flow cytometry with a Coulter Elite Laser. A total of 20,000 nuclei were counted from each sample. The percentages of cells within different cells stages were determined as described in the Materials and Methods. (**C**). Incorporation of [^{3}H] thymidine (5μCi/ml) into DNA of *L.donovani* (AG83) cells. Incorporation was monitored at different times after addition of [^{3}H] thymidine and 0.5% DMSO followed by the addition of DIM at 10, 20, 50 and 100 μM to the cell cultures (6.5 X 10^6 cells) at zero time. Aliquots of 50 μl

each were withdrawn from the cultures at the indicated time intervals and processed to determine the incorporation of label into acid-precipitable DNA. The experiments were performed three times and representative data from one set of these experiments are presented as means ± SD. Variations among different set of experiments were <5%.

Figure 10: Mitochondrial DNA depleted leishmanial cells (mtDDC) are insensitive to PCD in presence of DIM. (**A**). Cells were treated with 20 µM berenil for 24 h, washed with PBS and resuspended in M199 growing media in presence of 100 µg/ml pyruvate and 50 µg/ml uridine (mtDDC+P+U). These cells were allowed to grow for 12 h in presence of 0.2% DMSO (■) and 15 µM DIM (▲). Wild type cells were treated with 15 µM DIM for 12 h (◆). Percentage of viable parasites was measured by MTT assay. (**B**). Intracellular ATP level in mitochondrial DNA depleted parasites in presence (■) and absence (●) of pyruvate and uridine. The cells (mtDDC+P+U) were allowed to grow for 16 h in presence of 15 µM DIM (▲). (**C**). Intra-mitochondrial ROS generation in wild type parasites (WT) and mtDDC in presence of 15 µM DIM. (**D**). Fluorimetric analysis of mitochondrial membrane potential ($\Delta\Psi m$) in WT and mtDDC in presence of 15 µM DIM. The experiments were performed three times and representative data from one set of these experiments are expressed as mean ± SD. ***p<0.001 compared to WT plus DIM treatment with mtDDC plus DIM treatment.

Figure 11: Proposed model for DIM-induced programmed cell death in *Leishmania* parasites.

Molecular Pharmacology Fast Forward. Published on August 14, 2008 as DOI: 10.1124/mol.108.050161
This article has not been copyedited and formatted. The final version may differ from this version.

Table 1: Effect of DIM on Specific Activity of Respiratory Complexes

Mitochondrial Complexes of Electron Transport Chain	**Control (Untreated)**	**Specific Inhibitors of ETC (30 min)**	**DIM Treatment (15 µM)**	
			30 min	***120 min***
Complex I activity (nmol NADH oxidized/min/mg protein)	82.36 ± 9.2	2.51 ± 0.7 (Rotenone, 10 µM)	81.92 ± 6.6	62.83 ± 5.7
Complex II (Succinate-CoQ reductase activity/min/mg protein)	31.28 ± 2.7	5.45 ± 1.8 (TTFA, 10 µM)	30.81 ± 3.1	32.05 ± 2.6
Complex III (Cytocrome c-CoQ reductase activity/min/mg protein)	95.72 ± 9.4	6.12 ± 0.5 (Antimycin A, 10 µM)	95.26 ± 6.6	94.91 ± 7.2
Complex IV activity (nmol reduced cytocrome c oxidized/min/mg protein)	53.44 ± 3.1	4.59 ± 1.6 (Cyanide, 10 µM)	53.82 ± 3.5	52.94 ± 3.7
Complex V (ATP synthase activity/min/mg protein)	58.63 ± 7.4	9.96 ± 2.2 (Oligomycin, 10 µM)	09.98 ± 1.9	05.98 ± 0.6

Molecular Pharmacology Fast Forward. Published on August 14, 2008 as DOI: 10.1124/mol.108.050161
This article has not been copyedited and formatted. The final version may differ from this version.

Table 2: Specific Activity of Respiratory Complexes on mtDDC

Mitochondrial Complexes of Electron Transport Chain	**LDWT**	**mtDDC**
Complex I activity (nmol NADH oxidized/min/mg protein)	83.22 ± 3.8	2.33 ± 0.9
Complex II activity (Succinate-CoQ reductase activity/min/mg protein)	32.12 ± 3.3	30.27 ± 2.9
Complex III activity (Cytocrome c-CoQ reductase activity/min/mg protein)	93.28 ± 9.2	5.89 ± 0.4
Complex IV activity (nmol reduced cytocrome c oxidized/min/mg protein)	52.94 ± 2.9	5.12 ± 1.5
Complex V activity (ATP synthase activity/min/mg protein)	58.32 ± 6.5	9.22 ± 1.2

Figure 1

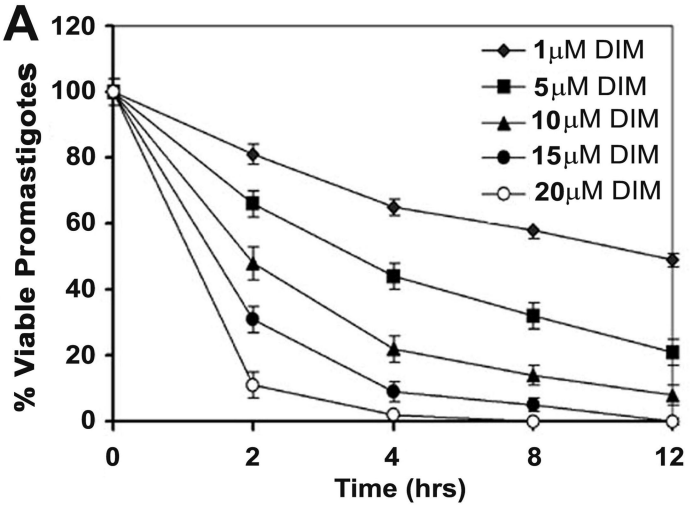
A
% Viable Promastigotes
120
100
80
60
40
20
0
0
2
4
8
12
Time (hrs)
1μM DIM
5μM DIM
10μM DIM
15μM DIM
20μM DIM

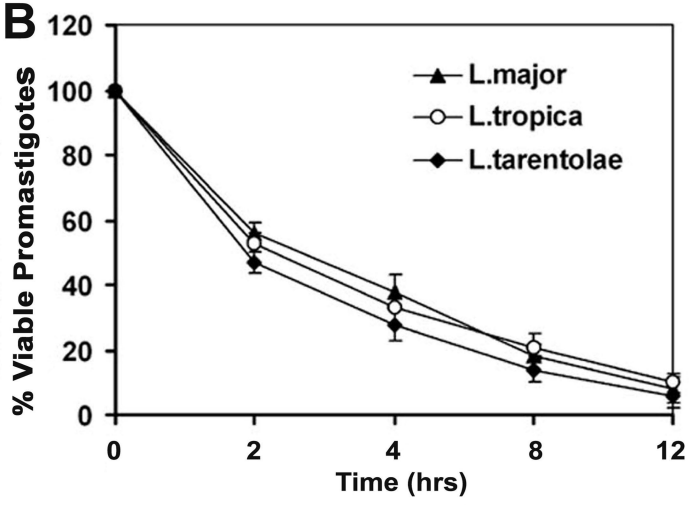
B
% Viable Promastigotes
120
100
80
60
40
20
0
0
2
4
8
12
Time (hrs)
L.major
L.tropica
L.tarentolae

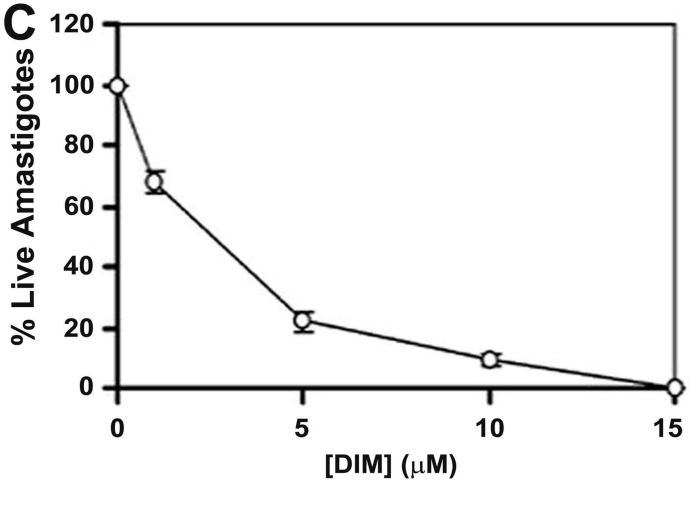
C
% Live Amastigotes
120
100
80
60
40
20
0
0
5
10
15
[DIM] (μM)

Figure 2

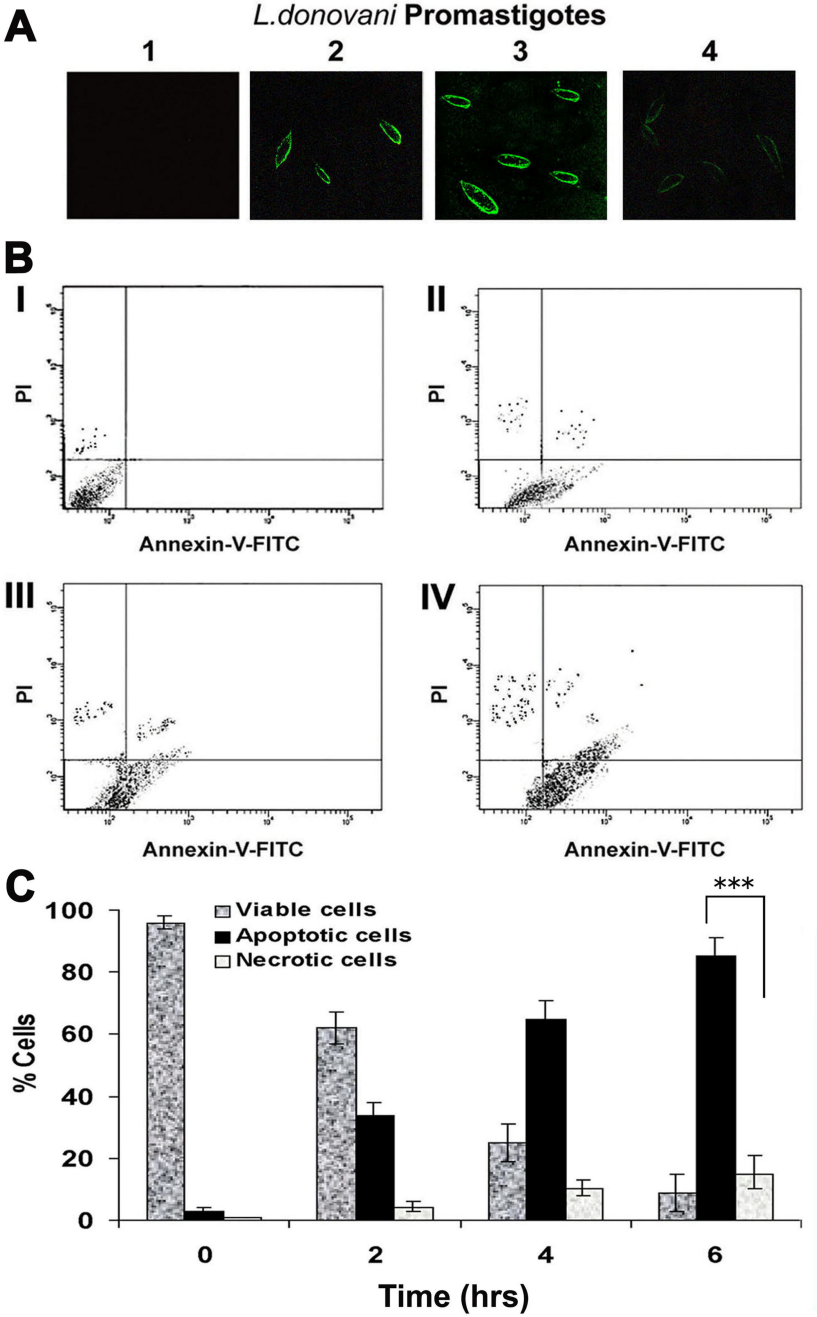
A
L.donovani Promastigotes
1
2
3
4
B
I
II
III
IV
PI
Annexin-V-FITC
C
Viable cells
Apoptotic cells
Necrotic cells
% Cells
100
80
60
40
20
0
***
0
2
4
6
Time (hrs)

Figure 3

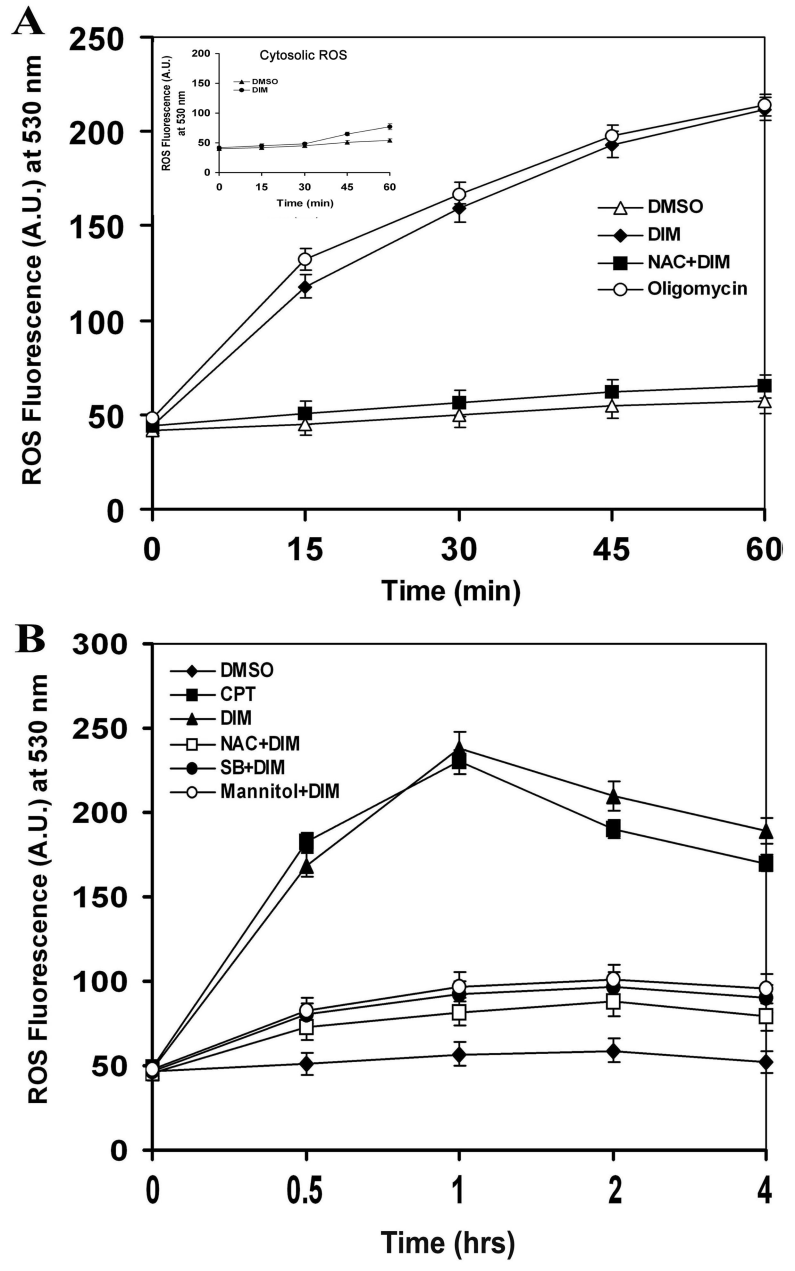
A
ROS Fluorescence (A.U.) at 530 nm
Time (min)
DMSO
DIM
NAC+DIM
Oligomycin
Cytosolic ROS
ROS Fluorescence (A.U.) at 530 nm
Time (min)
DMSO
DIM
B
ROS Fluorescence (A.U.) at 530 nm
Time (hrs)
DMSO
CPT
DIM
NAC+DIM
SB+DIM
Mannitol+DIM

Figure 4

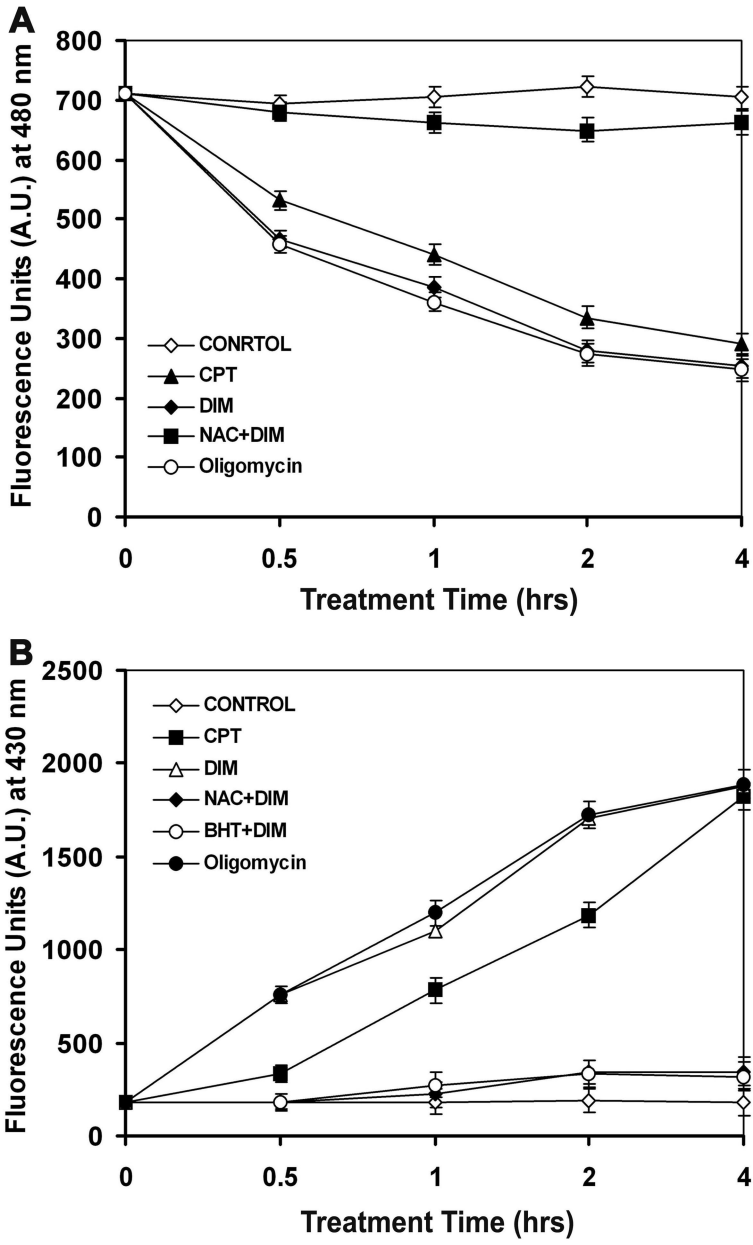
A
Fluorescence Units (A.U.) at 480 nm
800
700
600
500
400
300
200
100
0
CONRTOL
CPT
DIM
NAC+DIM
Oligomycin
0
0.5
1
2
4
Treatment Time (hrs)
B
Fluorescence Units (A.U.) at 430 nm
2500
2000
1500
1000
500
0
CONTROL
CPT
DIM
NAC+DIM
BHT+DIM
Oligomycin
0
0.5
1
2
4
Treatment Time (hrs)

Figure 5

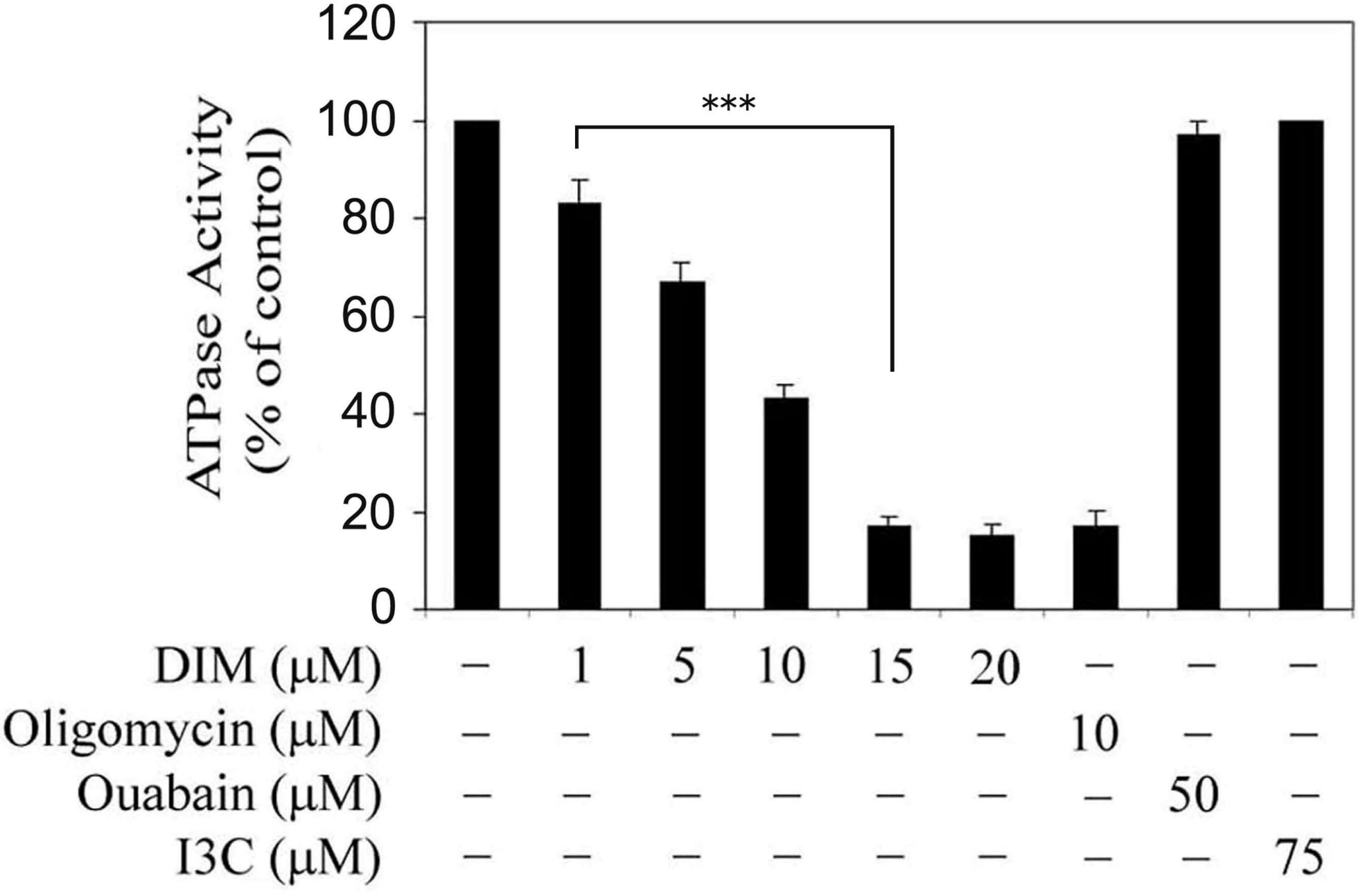
ATPase Activity
(% of control)
120
100
80
60
40
20
0
***
DIM (μM) – 1 5 10 15 20 – – –
Oligomycin (μM) – – – – – – 10 – –
Ouabain (μM) – – – – – – – 50 –
I3C (μM) – – – – – – – – 75

Figure 6

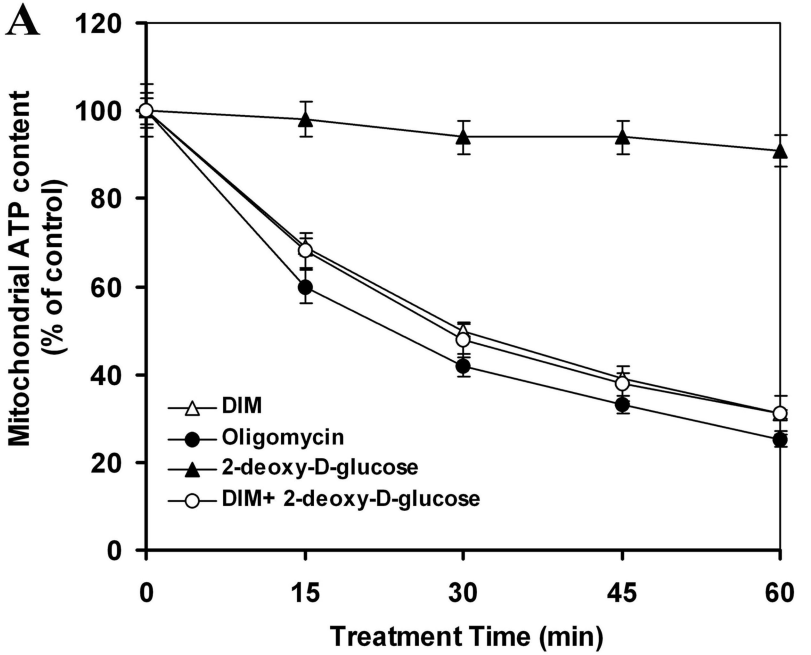
A
Mitochondrial ATP content
(% of control)
120
100
80
60
40
20
0
DIM
Oligomycin
2-deoxy-D-glucose
DIM+ 2-deoxy-D-glucose
0
15
30
45
60
Treatment Time (min)

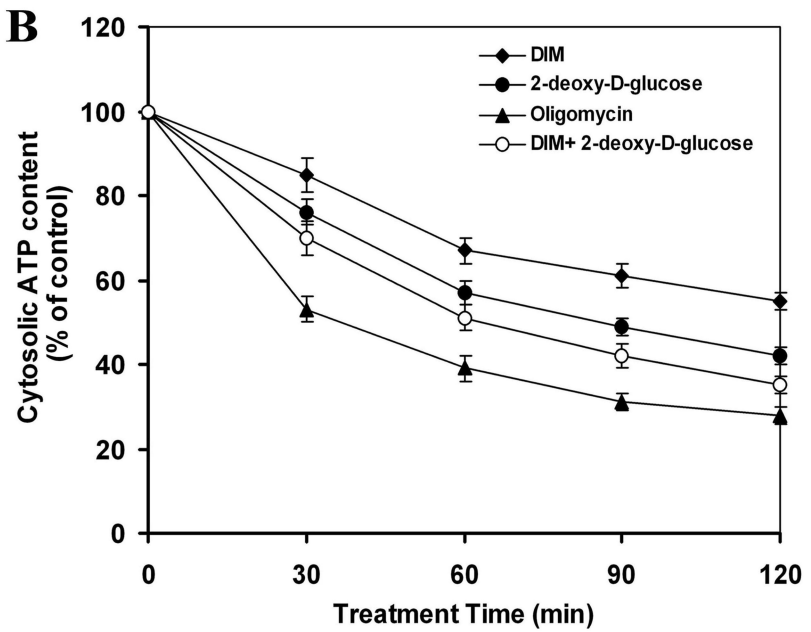
B
Cytosolic ATP content
(% of control)
120
100
80
60
40
20
0
DIM
2-deoxy-D-glucose
Oligomycin
DIM+ 2-deoxy-D-glucose
0
30
60
90
120
Treatment Time (min)

Figure 7

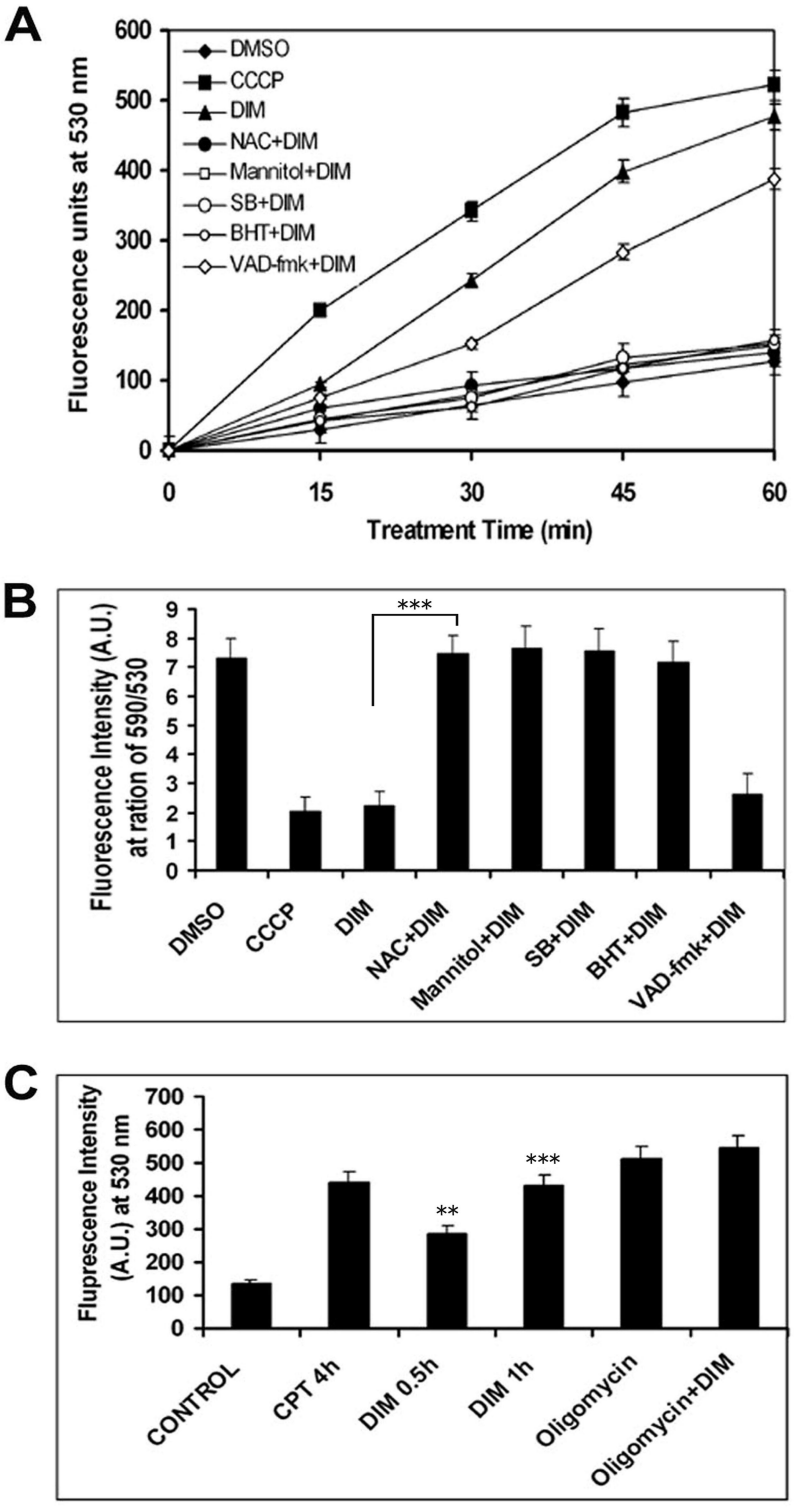
A
Fluorescence units at 530 nm
Treatment Time (min)
DMSO
CCCP
DIM
NAC+DIM
Mannitol+DIM
SB+DIM
BHT+DIM
VAD-fmk+DIM
B
Fluorescence Intensity (A.U.) at ration of 590/530
***
C
Fluprescence Intensity (A.U.) at 530 nm
**
***
CONTROL
CPT 4h
DIM 0.5h
DIM 1h
Oligomycin
Oligomycin+DIM

Figure 8

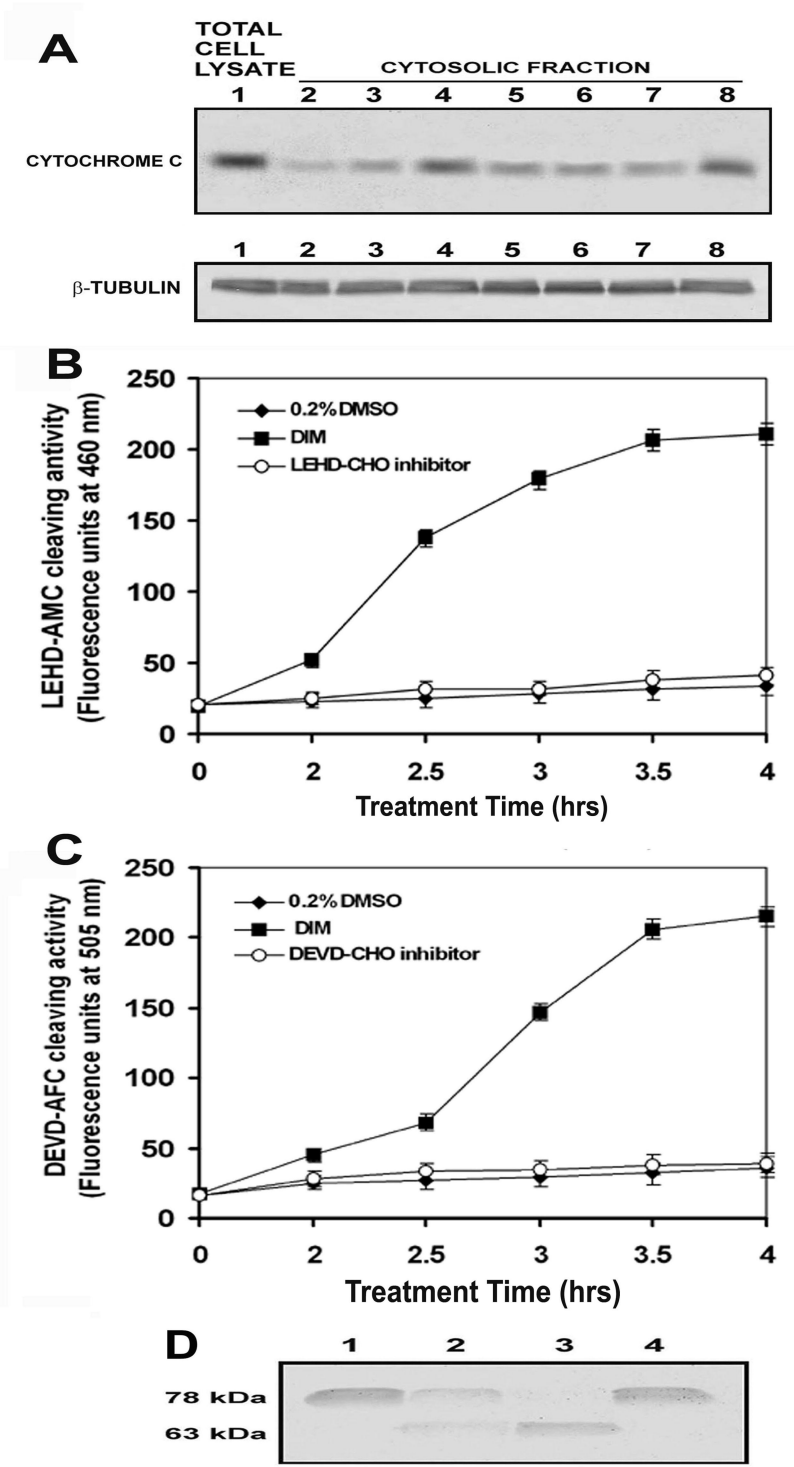
A
TOTAL CELL LYSATE
CYTOSOLIC FRACTION
1 2 3 4 5 6 7 8
CYTOCHROME C
1 2 3 4 5 6 7 8
β-TUBULIN
B
LEHD-AMC cleaving antivity (Fluorescence units at 460 nm)
0.2% DMSO
DIM
LEHD-CHO inhibitor
Treatment Time (hrs)
C
DEVD-AFC cleaving activity (Fluorescence units at 505 nm)
0.2% DMSO
DIM
DEVD-CHO inhibitor
Treatment Time (hrs)
D
1 2 3 4
78 kDa
63 kDa

Figure 9

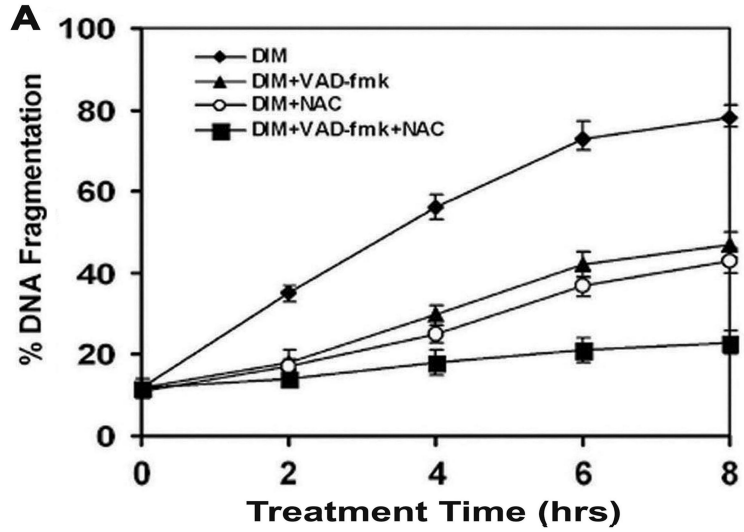
A
% DNA Fragmentation
DIM
DIM+VAD-fmk
DIM+NAC
DIM+VAD-fmk+NAC
Treatment Time (hrs)

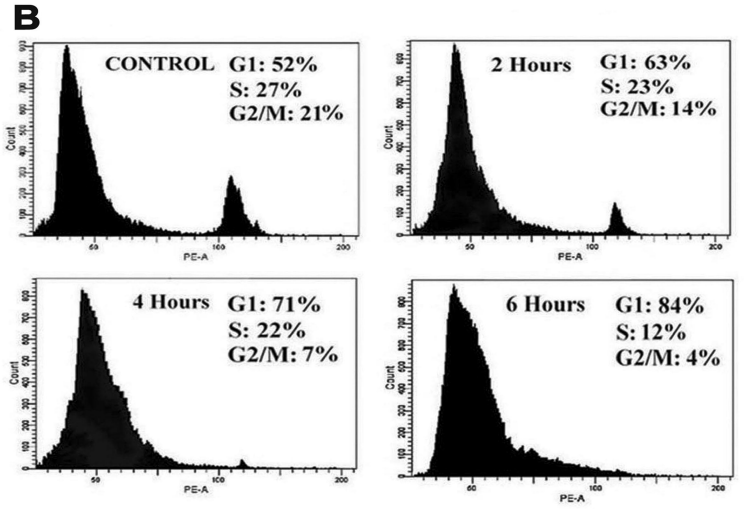
B
CONTROL G1: 52%
S: 27%
G2/M: 21%
2 Hours G1: 63%
S: 23%
G2/M: 14%
4 Hours G1: 71%
S: 22%
G2/M: 7%
6 Hours G1: 84%
S: 12%
G2/M: 4%
Count
PE-A

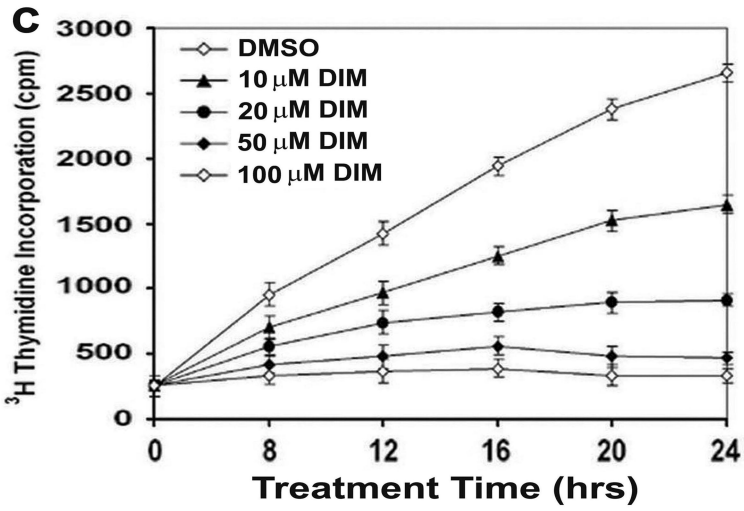
C
^{3}H Thymidine Incorporation (cpm)
DMSO
10 μM DIM
20 μM DIM
50 μM DIM
100 μM DIM
Treatment Time (hrs)

Figure 10

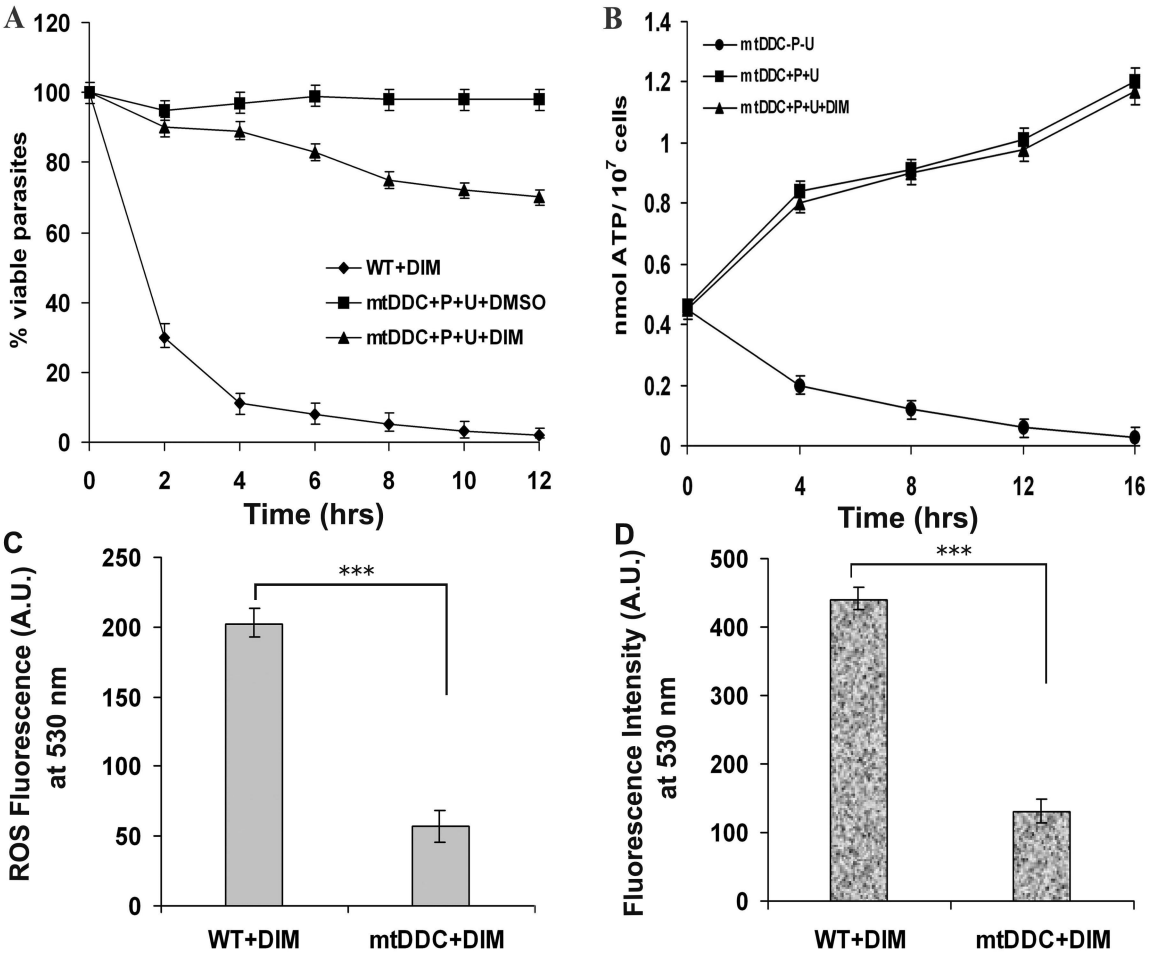
A
% viable parasites
Time (hrs)
WT+DIM
mtDDC+P+U+DMSO
mtDDC+P+U+DIM
B
nmol ATP/ 10^7 cells
Time (hrs)
mtDDC-P-U
mtDDC+P+U
mtDDC+P+U+DIM
C
ROS Fluorescence (A.U.) at 530 nm
***
WT+DIM
mtDDC+DIM
D
Fluorescence Intensity (A.U.) at 530 nm
***
WT+DIM
mtDDC+DIM

Figure 11

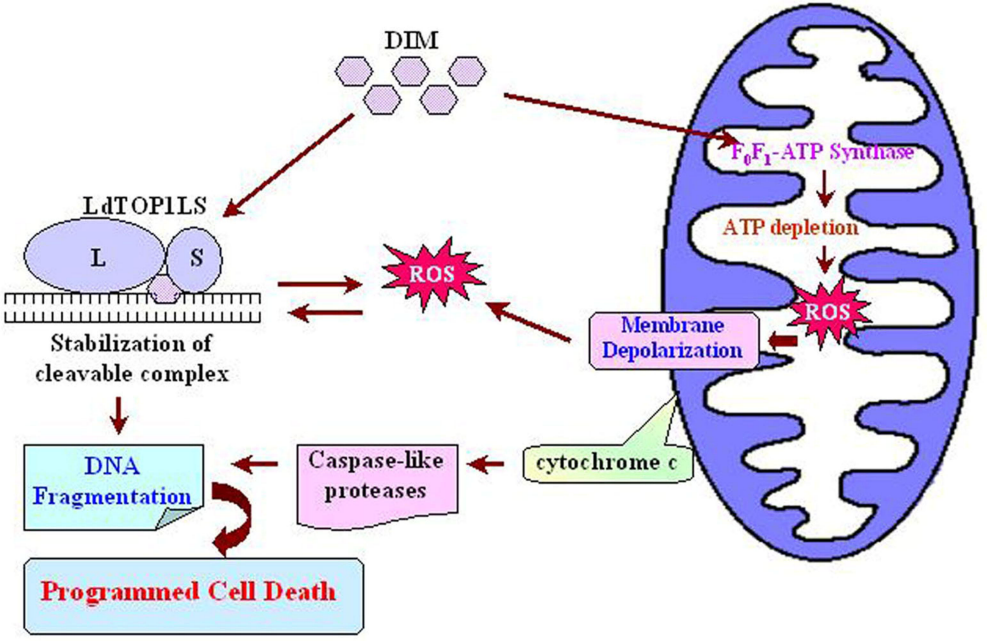
DIM
LdTOP1LS
L
S
Stabilization of cleavable complex
ROS
F_0F_1-ATP Synthase
ATP depletion
ROS
Membrane Depolarization
cytochrome c
Caspase-like proteases
DNA Fragmentation
Programmed Cell Death

SUPPLEMENTARY INFORMATION

Supplementary Methods:

Culture, differentiation and infection of U937 cells:

The human promonocytic cell line U937 was obtained from ATTC (American Type Culture Collection). Cells were cultured in suspension in stationary cell-culture flasks in RPMI-1640 medium (Sigma-Aldrich) supplemented with 10% FCS, penicillin and streptomycin at 37^0C in a humidified atmosphere of 5% CO_2 prior to infection with *L. donovani***,** U937 cells were cultured for 18 h in the presence of PMA (10 ng/ml; sigma), rendering the cells adherent and capable of phagocytosis of *L. donovani* promastigotes (Nandan et al., 1995). PMA-differentiated U937 cells were infected with freshly transformed promastigotes of *L.donovani* at a cell to parasite ratio of 1:10. After incubation at 37^0C for the 18 h, noningested parasites were removed by vigorous washing with RPMI-1640 medium three times. The infected macrophages (U937) were treated with different concentrations of DIM for 12 h. At least 400 macrophages were examined for each cover slip by Giemsa staining. Anti-leishmanial activity was determined by calculating the number of amastigotes per 100 macrophages.

Determination of *In vivo* parasites burden inhibition:

Female golden hamsters (4 wk, 60-80 gm/hamster) with 2 weeks after established infection were administered 10 mg and 20 mg/kg body weight of DIM by intramuscularly for 4 weeks before they were sacrificed. Control group received phosphate buffer saline (PBS). Liver and spleen parasitic loads were determined from impression smears after Giemsa staining. Experiments were carried out according to adequate ethical regulations. The results are expressed as the number of amastigotes/100 nuclei and the total parasitic load per organ, using the formula (Mittra et al., 2000):

Organ weight in mg X the number of amastigotes per nuclei X (2×10^5)

Supplementary Results:

DIM reduces the parasite burden in Liver and Spleen:

The inhibition of catalytic activities of DNA topoisomerases, growth of parasites and induction of apoptosis indicate that DIM is a highly potent anti-leishmanial agent. The therapeutic potential of DIM was further substantiated by an *in vivo* experiment. To carry out this experiment golden hamsters were infected with *L. donovani* AG83 promastigotes. Two weeks after infection the hamsters were treated with DIM (10 mg and 20 mg/kg body weight) for 4 weeks. Compared with the infected and untreated hamsters, which showed a progressive and fatal visceral leishmaniasis, when DIM at 20 mg/kg body weight was administered intramuscularly to the infected animals there was a reduction of 93% and 96% parasitic burden in liver and spleen respectively (Supplementary Fig. 1C and D). Giemsa-stained micrographs at liver and spleen smears for intramuscularly DIM-treated hamsters also show this profound effect and nearly complete reduction of parasitic burden (Supplementary Fig. 1B). DIM was found to be nontoxic as evident from the analysis of SGOT and SGPT of DIM treated animals. The weight of infected, untreated hamsters reduced drastically, compared with the weight of normal and DIM-treated infected hamsters, indicating healthy recovery. Infected organ (Liver and Spleen) weight of animals reduced at normal weight by DIM treatment (Supplementary Table 1 and 2).

Supplementary References:

Mittra B, Saha A, Chowdhury AR, Pal C, Mandal S, Mukhopadhyay S, Bandyopadhyay S and Majumder HK. (2000) Luteolin, an abundant dietary component is a potent anti-leishmanial agent that acts by inducing topoisomerase II-mediated kinetoplast DNA cleavage leading to apoptosis. *Mol Med.* **6:** 527-541.

Nandan D and Reiner NE. (1995) Attenuation of gamma interferon-induced tyrosine phosphorylation in mononuclear phagocytes infected with *Leishmania donovani*: selective inhibition of signaling through Janus kinases and Stat1. *Infect. Immun.* **63**: 4495-4500

Supplementary Legends for Figures:

Figure S1: DIM reduces parasites burden in macrophages (U937) and in animals.
(**A**). Micrographs of Giemsa-stained of the infected macrophages (U937) with *L. donovani* AG83 promastigotes and incubated with 5 and 10 µM of DIM and 10 µM of SAG as positive control as indicated in Figure. (**B**). Micrographs of Giemsa-stained hepatic and splenic smears of *L. donovani*-infected golden hamsters after treatment with DIM and SAG as a positive control. (**C** and **D**). DIM reduces the both hepatic and splenic parasites burden in infected golden hamsters. Experiments with intramuscular administration of DIM and SAG were performed in triplicate and representative data from one set of these experiments for liver and spleen are expressed as mean ± SD.

Figure S2: Characterization of mtDDC.
Confocal microscopy of kDNA loss in *L.donovani* wild type parasites and mtDDC. The parasites were stained with EtBr (0.1 µg/ml) in PBS (1X) containing 10% glycerol. Right column indicates the fluorescence-labeled cells viewed with a Leica confocal microscope. Left column indicates the merged pictures of fluorescence and phase contrast microscope. Magnification X100. Pictures are representative from one of three similar studies. N indicates to nucleus and K indicates to kinetoplast.

Supplementary Table 1

Groups	Organ weight (LIVER)	No. Of Amastigotes/ 100 Nuclei	Total parasites loading [*Organ wt. in mg X No. Of Amastigotes/Nucleus* X *(2X10^5)*]	Total % Of Inhibition
Infected control	5950 mg	185	5950x1.85x*(2X10^5)* **=22.02 x10^8**	00
SAG Control (20 mg/kg)	4530 mg	15	4530x0.15x*(2X10^5)* **=1.36 x10^8**	**94%**
DIM (10 mg/kg)	5024 mg	59	5024x0.59x*(2X10^5)* **=5.93 x10^8**	73%
DIM (20 mg/kg)	4668 mg	16	4668x0.16x*(2X10^5)* **=1.49 x10^8**	**93%**

Supplementary Table 2

Groups	Organ weight (SPLEEN)	No. Of Amastigotes/ 100 Nuclei	Total parasites loading [*Organ wt. in mg X No. Of Amastigotes/Nucleus* X *(2X10^5)*]	Total % Of Inhibition
Infected control	730 mg	240	730x2.40x*(2X10^5)* **=3.50 x10^8**	00
SAG Control (20 mg/kg)	420 mg	14	420x0.14x*(2X10^5)* **=0.12x10^8**	**97%**
DIM (10 mg/kg)	572 mg	56	572x0.56x*(2X10^5)* **=0.64 x10^8**	82%
DIM (20 mg/kg)	424 mg	18	424x0.18x*(2X10^5)* **=0.15 x10^8**	**96%**

Supplementary Figure 1:

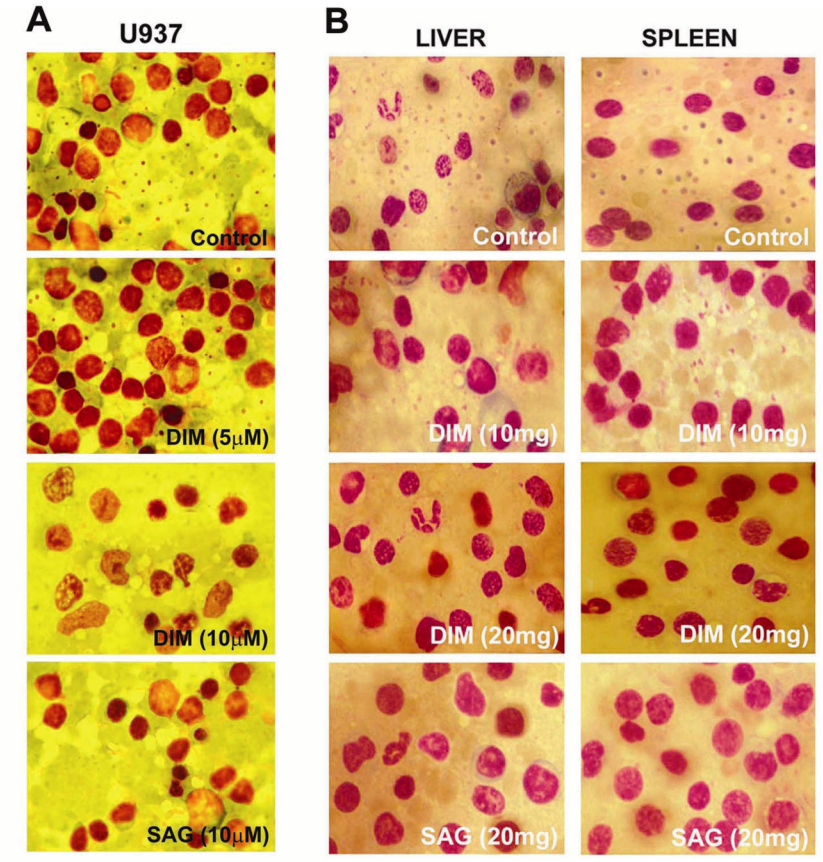

C

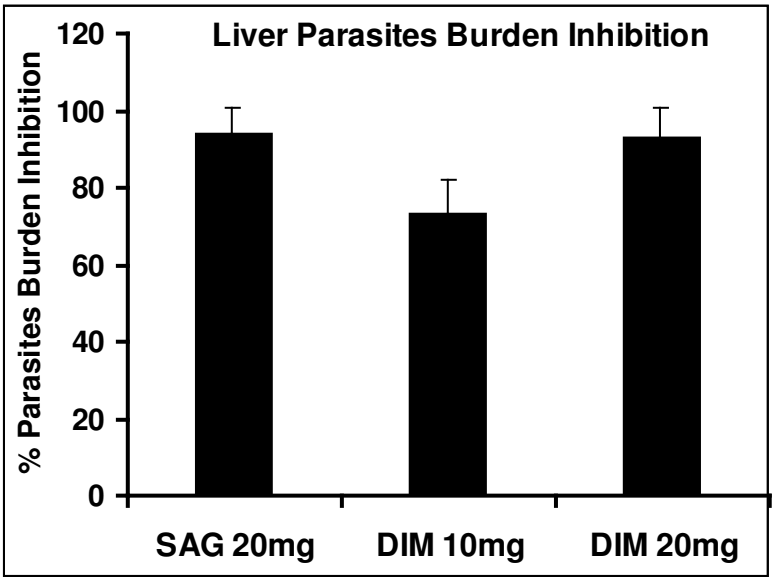
Liver Parasites Burden Inhibition
% Parasites Burden Inhibition
120
100
80
60
40
20
0
SAG 20mg
DIM 10mg
DIM 20mg

D

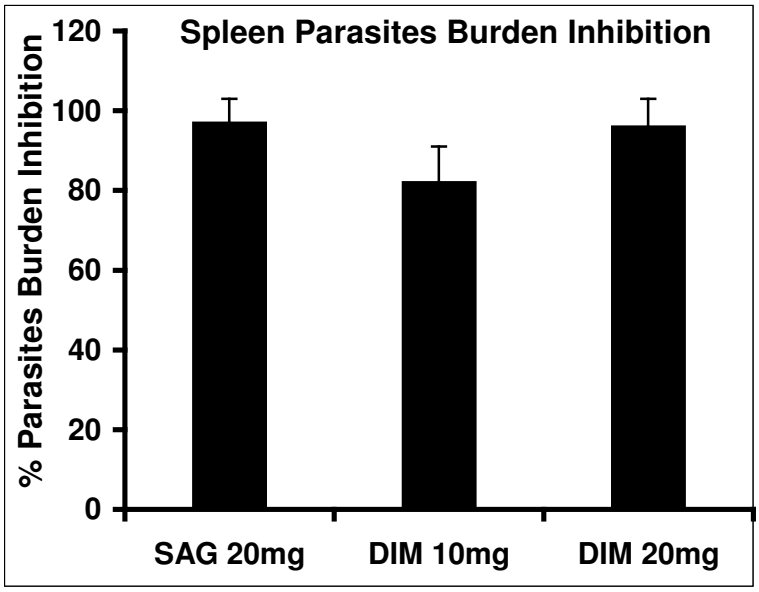
Spleen Parasites Burden Inhibition
% Parasites Burden Inhibition
120
100
80
60
40
20
0
SAG 20mg
DIM 10mg
DIM 20mg

Supplementary Figure 2: